Accepted Manuscript

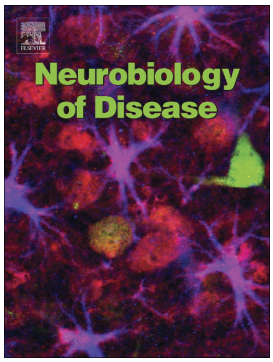

Toxicity and aggregation of the polyglutamine disease protein, ataxin-3 is regulated by its binding to VCP/p97 in Drosophila melanogaster

Gorica Ristic, Joanna R. Sutton, Kozeta Libohova, Sokol V. Todi

PII: S0969-9961(18)30121-9
DOI: doi:10.1016/j.nbd.2018.04.013
Reference: YNBDI 4154

To appear in: *Neurobiology of Disease*

Received date: 21 December 2017
Revised date: 26 March 2018
Accepted date: 22 April 2018

Please cite this article as: Gorica Ristic, Joanna R. Sutton, Kozeta Libohova, Sokol V. Todi , Toxicity and aggregation of the polyglutamine disease protein, ataxin-3 is regulated by its binding to VCP/p97 in Drosophila melanogaster. The address for the corresponding author was captured as affiliation for all authors. Please check if appropriate. Ynbdi(2017), doi:10.1016/j.nbd.2018.04.013

Toxicity and aggregation of the polyglutamine disease protein, ataxin-3 is regulated by its binding to VCP/p97 in *Drosophila melanogaster*

Gorica Ristic[#,1,&], Joanna R. Sutton[#,1], Kozeta Libohova[1], Sokol V. Todi[1,2,§]

#- These authors contributed equally to this manuscript

1- Department of Pharmacology, Wayne State University School of Medicine, Detroit, MI USA

2- Department of Neurology, Wayne State University School of Medicine, Detroit, MI USA

&- Present address: Department of Pathology, University of Michigan Medical School, Ann Arbor, MI USA

§- Correspondence: 540 E Canfield, Scott Hall Rm. 3108, Detroit, MI 48201, USA. stodi@wayne.edu

Keywords: AAA ATPase; ataxia; ataxin-3; deubiquitinase; Machado-Joseph Disease; neurodegeneration; polyglutamine; Spinocerebellar Ataxia Type 3; VCP/p97

ABSTRACT

Among the nine dominantly inherited, age-dependent neurodegenerative diseases caused by abnormal expansion in the polyglutamine (polyQ) repeat of otherwise unrelated proteins is Spinocerebellar Ataxia Type 3 (SCA3). SCA3 is caused by polyQ expansion in the deubiquitinase (DUB), ataxin-3. Molecular sequelae related to SCA3 remain unclear. Here, we sought to understand the role of protein context in SCA3 by focusing on the interaction between this DUB and Valosin-Containing Protein (VCP). VCP is bound directly by ataxin-3 through an arginine-rich area preceding the polyQ repeat. We examined the importance of this interaction in ataxin-3-dependent degeneration in *Drosophila melanogaster*. Our assays with new isogenic fly lines expressing pathogenic ataxin-3 with an intact or mutated VCP-binding site show that disrupting the ataxin-3-VCP interaction delays the aggregation of the toxic protein *in vivo*. Importantly, early on flies that express pathogenic ataxin-3 with a mutated VCP-binding site are indistinguishable from flies that do not express any SCA3 protein. Also, reducing levels of VCP through RNA-interference has a similar, protective effect to mutating the VCP-binding site of pathogenic ataxin-3. Based on *in vivo* pulse-chases, aggregated species of ataxin-3 are highly stable, in a manner independent of VCP-binding. Collectively, our results highlight an important role for the ataxin-3-VCP interaction in SCA3, based on a model that posits a seeding effect from VCP on pathogenic ataxin-3 aggregation and subsequent toxicity.

INTRODUCTION

Spinocerebellar Ataxia Type 3 (SCA3, or Machado-Joseph Disease) is an age-related, neurodegenerative disease that is considered to be the most common, dominantly inherited ataxia in the world (Costa Mdo and Paulson, 2012; Todi et al., 2007b). SCA3 belongs to the family of polyglutamine (polyQ) diseases along with five other SCAs (1, 2, 6, 7 and 17), Huntington's Disease, Kennedy's Disease, and Dentatorubropallidoluysian Atrophy (Costa Mdo and Paulson, 2012; Matos et al., 2011; Todi et al., 2007b). These diseases are characterized by abnormally expanded CAG triplet repeats in the respective genes, which lead to expanded polyQ tracts in their proteins. Expanded polyQ repeats in these proteins cause their misfolding and the formation of insoluble aggregates (Costa Mdo and Paulson, 2012; Matos et al., 2011; Todi et al., 2007b). SCA3 is caused by an expansion of the CAG repeat of the *ATNX3* gene, which encodes the protein ataxin-3 (figure 1A). There is no cure for SCA3.

Ataxin-3 is a deubiquitinating enzyme (DUB) that has been linked to protein quality control with various partners (Costa Mdo and Paulson, 2012; Reina et al., 2012; Scaglione et al., 2011). One such partner is Valosin-Containing Protein (VCP, also known as p97), a member of the AAA (ATPases Associated with diverse cellular Activities) family of proteins (figure 1B; Meyer et al., 2012). VCP functions as a homohexamer, converting chemical energy harvested from ATP hydrolysis to mechanical energy to exert force on its substrates. It is an essential, ubiquitously expressed protein involved in numerous cellular processes, including protein degradation (Xia et al., 2016).

Ataxin-3 binds VCP directly (Doss-Pepe et al., 2003; Hirabayashi et al., 2001; Wang et al., 2006) through a region on its C-terminal half (figure 1A; Boeddrich et al.,

2006). According to biochemical and cell-based experiments from an elegant study by the Wanker and Bonini labs, ataxin-3 binds to the N-terminal portion of VCP through an arginine-rich area (amino acid sequence RKRR; Boeddrich et al., 2006; figure 1A). Mutating the VCP-binding site on ataxin-3 disrupts the interaction between these two proteins (Boeddrich et al., 2006). The same study also showed that recombinant VCP stimulates fibrillogenesis/aggregation of recombinant, pathogenic ataxin-3 in a dose-dependent manner in reconstituted systems, but only up to a point; molar excess VCP suppresses ataxin-3 fibrillogenesis. These results suggested a seeding role for VCP: the hexamer binds multiple ataxin-3 proteins, increasing their chances of interacting together and enhancing their initial aggregation (Boeddrich et al., 2006). Exogenous VCP mitigated, to some extent, degeneration caused by full-length, pathogenic ataxin-3 in one tissue tested, the eyes of fruit flies (Boeddrich et al., 2006). These compelling data highlight the need for additional examinations to understand the interaction between ataxin-3 and VCP *in vivo*. Direct comparison between pathogenic ataxin-3 that can bind VCP and a version that has the VCP-binding site mutated—expressed similarly in various tissues—is necessary to appreciate the interplay between these proteins in SCA3. It would also help overall understanding of SCA3 biology to examine if VCP regulates the aggregative propensity of pathogenic ataxin-3 in an intact animal, beyond *in vitro* settings. Lastly, examining the relationship of the VCP-ataxin-3 interaction to the temporal aggregation and pathogenicity of the SCA3 protein in an intact animal would be helpful both to further our knowledge of SCA3 disease mechanisms, and to determine if this interaction could be of therapeutic benefit. These were the various aspects that we set out to tackle in this work, by using *Drosophila* as a model organism.

We generated isogenic lines of *Drosophila melanogaster* that express, in a Gal4-UAS-dependent manner (Brand et al., 1994; Brand and Perrimon, 1993), full-length, human, pathogenic ataxin-3 with a normal or mutated VCP-binding site. We found that pathogenic ataxin-3 with mutated VCP-binding is markedly less toxic and less aggregation-prone in flies, even though the protein is present at levels similar to its VCP-binding counterpart. Also, altering the levels of endogenous VCP protein modulates the toxicity of the SCA3 protein. Our data highlight an important physiological role for VCP on ataxin-3-dependent degeneration, and underscore the importance of non-polyQ regions of this DUB to the toxicity of its expanded repeat.

MATERIALS AND METHODS

Drosophila Lines: Husbandry was conducted at 25˚C on standard cornmeal food at 40-60% humidity in regulated diurnal environments. SCA3 flies expressing pathogenic ataxin-3 with 77-80 polyQ repeats were previously generated by cloning into the pWalium10-moe vector (Sutton et al., 2017). "HNHH" mutation was generated on the ataxin-3 backbone using the QuikChange mutagenesis kit (Aglient) and this construct was cloned into the pWalium10-moe vector to create "HNHH" pathogenic ataxin-3-encoding flies. Injections (Duke University Model Systems) were into y,w;+;attP2. Common fly stocks were procured from the Bloomington *Drosophila* Stock Center: GMR-Gal4 (#8121), isogenic host strain attP2 (#36303), VCP RNAi lines (#32869, #35608). The HA-tagged VCP line was #F001765 from FlyORF. The following lines were gifts: sqh-Gal4 driver (Dr. Daniel P. Kiehart, Duke University), elav-Gal4(GS) driver (Dr. R. J. Wessells, Wayne State University), elav-Gal4 driver (Dr. Daniel F. Eberl, University of Iowa).

Longevity Assay: Approximately 25 adult flies per vial were collected after eclosion from the pupal case and aged on conventional cornmeal fly media or RU-486-containing media (Nicholson et al., 2008; Osterwalder et al., 2001; Roman and Davis, 2002; Sujkowski et al., 2015) at 25°C. Flies were switched to vials with fresh food every 2-3 days. Each vial was examined for death daily, until all flies were dead.

Motility Assay (Negative Geotaxis): Motility was tested once a week for a total of four weeks. Ten flies per vial were forced to the bottom of the vial by light tapping on the

bench. The number of flies that reached the top of the vial at 5, 15 and 30 seconds was recorded. Flies were transferred to new vials 1 hour before assessment, and every 2-3 days for the duration of the experiment.

Ataxin-3 Pulse-Chases in Drosophila: Fly crosses were set up in standard cornmeal media under the conditions described in "*Drosophila* Lines". After eclosion, adult offspring possessing transgenes for the inducible elav-Gal4(GS) driver and UAS-Ataxin-3(SCA3)-Intact or UAS-Ataxin-3(SCA3)-HNHH were transferred to cornmeal media containing RU-486 (Roman and Davis, 2002; Sujkowski et al., 2015). Expression of UAS-Ataxin-3(SCA3)-Intact was induced in the RU-486-containing media for 7 or 14 days; expression of UAS-Ataxin-3(SCA3)-HNHH was induced for 10 or 21 days. At the end of the induction period, flies were transferred back to the standard cornmeal media for a chase period of 14 or 21 days. Longevity, motility and western blot analyses were carried out as described in the rest of the Materials and Methods section.

Histology: Fly proboscises and wings were removed before fixing overnight in 2% glutaraldehyde/2% paraformaldehyde in Tris-buffered saline with 0.1% Triton X-100. Fixed flies were dehydrated in a series of 30, 50, 70, 100% ethanol washes for 1 hour each, then washed in propylene oxide overnight. Whole fly bodies were embedded in Poly/Bed812 (Polysciences), sectioned at 5 µm, and stained with toluidine blue.

Western Blotting and quantifications: Five whole flies or 15 dissected fly heads per group were homogenized in hot lysis buffer (50mM Tris pH 6.8, 2% SDS, 10% glycerol,

100mM dithiothreitol), sonicated, boiled for 10 minutes, and centrifuged at top speed at room temperature for 10 minutes. Samples were electrophoresed on 4-20% gradient gels (BioRad). Western blots were developed using the charge-coupled device-equipped VersaDoc 5000MP system (BioRad). Blots were quantified using Quantity One software (BioRad). The signal for SDS-resistant ataxin-3 species above the dotted lines in each shown blot and from independent repeats was divided by the total ataxin-3 signal (SDS-Soluble + SDS-Resistant) for that specific lane and expressed as a percentage. For direct blue staining, PVDF membranes were submerged for 5 minutes in 0.1% Direct Blue 71 (Sigma-Aldrich) stock solution in ultrapure water, dissolved in 40% ethanol and 10% acetic acid solvent. Membrane was rinsed briefly in solvent, then ultrapure water, air dried, and imaged.

Antibodies: Anti-Ataxin-3 (mouse monoclonal 1H9, 1:500-1,000; Millipore) (rabbit polyclonal, 1:15,000; (Paulson et al., 1997)), anti-tubulin (mouse monoclonal T5168, 1:10,000; Sigma-Aldrich), anti-VCP (rabbit monoclonal,1:1,000; Cell Signaling Technology), anti-HA (rabbit monoclonal, 1:500-1,000; Cell Signaling Technology), anti-lamin (mouse monoclonal ADL84.12-5, 1:1,000; Developmental Studies Hybridoma Bank), peroxidase conjugated secondary antibodies (goat anti-mouse and goat anti-rabbit, 1:5,000; Jackson Immunoresearch)

Differential Centrifugation: Five whole flies per group were lysed in 200 µL of NETN buffer (50 mM Tris, pH 7.5, 150 mM NaCl, 0.5% Nonidet P-40), supplemented with protease inhibitor cocktail (PI, SigmaFast Protease Inhibitor Cocktail Tablets), sonicated,

and centrifuged at 20,000 x g for 30 minutes at 4˚C. The supernatant was transferred to a new tube and quantified by the BCA assay (Thermo Scientific). The pellet was resuspended in 200 µL of PBS + 1% SDS, vortexed, and boiled. Ten µg of the supernatant fraction and 7 µL of the pellet fraction were supplemented with 6x SDS, boiled, and loaded onto 4-20% gradient gels for western blot analysis.

Nuclear Cytoplasmic Extraction: Experiments were conducted using the ReadyPrep Protein Extraction Kit (Cytoplasmic/Nuclear; BioRad) to enrich cytoplasmic and nuclear proteins. Five whole adult flies were lysed in cytoplasmic extraction buffer (BioRad). Nuclei were resuspended in Protein Solubilization Buffer (BioRad). Samples were analyzed by western blot.

Quantitative PCR: Total RNA was extracted from whole adult flies using TRIzol (Life Technologies). Extracted RNA was treated with TURBO DNAse (Ambion). Reverse transcription was carried out using the high capacity cDNA reverse transcription kit (ABI). mRNA levels were quantified using the StepOne Real-Time PCR system with Fast SYBR Green Master Mix (ABI).

Primers:

SCA3 F: 5’-GAATGGCAGAAGGAGGAGTTACTA- 3’

SCA3 R: 5’-GACCCGTCAAGAGAGAATTCAAGT- 3’

rp49 F: 5’ -AGATCGTGAAGAAGCGCACCAAG- 3’

rp49 R: 5’ -CACCAGGAACTTCTTGAATCCGG- 3’

Cell Lines, Plasmids, and Transfection: HEK293 cells were purchased from ATCC and cultured in DMEM supplemented with 10% FBS and 5% Penicillin-Streptomycin, under conventional conditions. The day before transfection, cells were seeded in 6-well plates. For each condition, 3 wells were transfected using Lipofectamine LTX (Invitrogen) as instructed by the manufacturer. Twenty-four hours after transfection, cells were harvested in PBS (1 mL per well), pelleted by centrifugation at 500 x g for 5 minutes at 4˚C, and frozen at -80˚C. Ataxin-3 constructs were in pFLAG-CMV-6a. VCP construct was in pEGFP.

Co-Immunoprecipitation: For co-IPs from fly lysates, 30-50 fly heads per group were homogenized through mechanical disruption in PBS + PI, briefly sonicated, and then supplemented with the equal volume of NETN + PI. Lysates were vortexed briefly every 5 minutes for a total of 30 minutes, centrifuged at 5,000 x g for 5 minutes at 4˚C, and supernatant was transferred to 30 µL slurry of anti-HA bead-bound antibody (Sigma-Aldrich). Beads with lysates were tumbled at 4˚C for 4 hours. For co-IPs from cell lysates, HEK293 cells were transfected and harvested as described under “Cell Lines, Plasmids, and Transfections”. Cell pellets were lysed in 500 mL of NETN+PI, vortexed briefly every 5 minutes for a total of 30 minutes, and centrifuged at 12,000 x g for 15 minutes at 4˚C. Supernatants were transferred to 30 µL slurry of anti-FLAG bead-bound antibody (Sigma-Aldrich). Beads with lysates were tumbled at 4˚C for 4 hours. For *in vitro* pulldowns, 1.5 mL of bacterial lysate containing GST, GST-Ataxin-3(SCA3)-Intact, or GST-Ataxin-3(SCA3)-HNHH was tumbled with 20 µL of glutathione sepharose slurry for 30 minutes. Both Ataxin-3(SCA3) constructs contained 80 polyQ repeats. GST-

Ataxin-3(SCA3)-Intact and Ataxin3(SCA3)-HNHH supernatants were replaced with 1.5 mL of fresh bacterial lysate before tumbling all lysates for an additional 30 minutes. Forty whole flies were homogenized in 500 µL of NETN + PI, sonicated, and centrifuged at 15,000 x g for 15 minutes at 4˚C. The bacterial lysate was removed from the beads, beads were rinsed with NETN + PI, the fly lysate was distributed evenly among the 3 experimental groups, and samples were tumbled for 2 hours at 4˚C. Bead-bound complexes from all co-precipitations were rinsed thrice with NETN + PI, then eluted by boiling in Laemmli buffer.

Protein Purification: Glycerol stocks of BL21 cells transformed with pGEX6p1, pGEX6p1-Ataxin-3(SCA3)-Intact, or pGEX6p1-Ataxin-3(SCA3)-HNHH were used to inoculate 10 mL of LB + 50 µg/mL ampicillin. Both Ataxin-3(SCA3) constructs contained 80 polyQ repeats. Cultures were grown overnight at 37˚C, then used to inoculate 500 mL of LB + ampicillin, which was grown for an additional 1.5 hours to OD_{600}=0.60. Protein expression was induced with 0.5 mM of isopropyl-1-β-D-galactopyranoside (A. G. Scientific) for 4 h at 30°C. Bacterial cells were pelleted by centrifugation at 4,500 x g for 10 minutes at 4°C. Pellets were lysed in NETN buffer, sonicated, centrifuged, aliquoted, and frozen at -80°C.

RESULTS

Mutating the VCP-binding site of ataxin-3 disrupts its interaction with VCP in flies

We began our journey into the role of the VCP-ataxin-3 interaction in SCA3-like degeneration in *Drosophila* by confirming that the VCP-binding site mutation, “RKRR” to “HNHH", disrupts the DUB’s interaction with fly VCP. This mutation was shown before to interrupt binding of recombinant ataxin-3 to mammalian VCP (Boeddrich et al., 2006). We generated recombinant, pathogenic ataxin-3 with 80 polyQ in bacterial cells. This repeat is within patient range. We produced two versions of the DUB: one that has the intact VCP-binding site and one whose site is mutated, “RKRR” → "HNHH". We then incubated bead-bound, GST-tagged, recombinant ataxin-3 with whole fly lysate and probed for the ability of human ataxin-3 to interact with fly VCP. As shown in figure 1C, the pathogenic version of ataxin-3 co-precipitates fly VCP, whereas the version with mutated VCP-binding has a markedly reduced capacity to bind fly VCP; the western blot signal was barely above non-specific background (figure 1C). This disruption in interaction between VCP and ataxin-3 is similar to what we observe in mammalian cells: pathogenic ataxin-3 with impaired VCP-binding is unable to co-IP human VCP beyond non-specific background, whereas pathogenic ataxin-3 with intact VCP-binding co-IPs this interactor (figure 1D). In figures 1C and 1D, we used mild conditions that brought down some VCP non-specifically, which helped us to not exclude the possibility of residual VCP interaction with VCP-binding-mutated ataxin-3. Lastly, as shown in figure 1E, mutating the RKRR region on pathogenic ataxin-3 removes its ability to bind fly VCP *in vivo*. In this last setup, we co-expressed HA-tagged, fly VCP alongside ataxin-3 in *Drosophila* eyes and precipitated VCP. HA-VCP co-IPs pathogenic ataxin-3 with an intact

VCP-binding site, but not the pathogenic version with the “HNHH" mutation (figure 1E). We conclude that this specific mutation on pathogenic ataxin-3 effectively disrupts the interaction of the SCA3 protein with *Drosophila* VCP.

Mutating the VCP-binding site of ataxin-3 does not alter its mRNA levels or sub-cellular localization

We have at hand flies that express pathogenic ataxin-3 with an intact or mutated VCP-binding site. We generated the full-length, human, pathogenic ataxin-3 for earlier work (Sutton et al., 2017). For the present work, we created new transgenic *Drosophila* lines expressing ataxin-3 with 80 polyQ repeats with the “RKRR” to “HNHH" mutation. The new lines were constructed by cloning this ataxin-3 transgene into the pWalium10-moe vector, which was used with the phiC31 site-specific integrase system to insert a single copy of the construct at the attP2 site on the third chromosome of the fly, in the same orientation (Groth et al., 2004; Tsou et al., 2016). These flies are referred to as "HNHH" 1 and 2, as we utilized two independently derived lines, which ultimately led to the same results that were combined in most figures. The “HNHH" lines are isogenic to the “In-tact” SCA3 line.

First, we wanted to confirm that any difference in phenotype we might observe among the different lines is not due to a change in ataxin-3 transgene expression levels. We examined mRNA expression levels of ataxin-3 by qRT-PCR when the transgenes were expressed in the whole fly using the ubiquitous driver, sqh-Gal4 (figure 1F). There is no statistically significant difference in the expression levels of ataxin-3 among the three fly lines. Our lab also reported previously that ataxin-3 turnover is not affected

when the VCP-binding site was mutated in mammalian cells (Blount et al., 2014) or in *Drosophila* (Tsou et al., 2015).

The VCP-binding site on ataxin-3 is an arginine-rich region located at the C-terminus of ataxin-3. Previously, this domain was thought to encode a nuclear localization signal (Albrecht et al., 2004). We examined whether mutating the VCP-binding site affects the localization of pathogenic ataxin-3, using centrifugal fractionation of whole-fly lysates. We observed no difference in ataxin-3's distribution between the cytoplasm and nucleus when the VCP-binding site is mutated (figure 1G). We conclude that mutating the VCP-binding site from "RKRR" to "HNHH" does not impact the cellular localization of pathogenic ataxin-3 in the fly.

Mutating the VCP-binding site of pathogenic ataxin-3 reduces its toxicity in flies

To physiologically assess how mutating the VCP-binding site affects the toxicity of ataxin-3 in *Drosophila,* we conducted longevity studies. As we showed previously (Sutton et al., 2017), pathogenic ataxin-3 is highly toxic to the fly when it is expressed ubiquitously. We observe death during late pharate adult stages, during eclosion from the pupal case, and shortly following eclosion (figure 2A). Those flies that successfully eclose survive for about 30 days (figure 2B). As a frame of reference, flies not expressing pathogenic ataxin-3 can live up to ~90 days (Sutton et al., 2017). "HNHH" mutant flies all reach adulthood (figure 2A). We did not observe death during development as we had with flies encoding ataxin-3 with intact VCP-binding. From longevity data, we observed a clear separation in the rates of death early on: the "HNHH" mutant-expressing flies appear healthier and more flies remain alive in the earlier days of life than their "Intact"

ataxin-3-expressing counterparts (figure 2B). The longevity curves for “HNHH” lines 1 and 2 were nearly indistinguishable from one another (supplemental figure 1); thus, they were combined in this and the rest of the longevity assays in this report. When compared with the control flies that do not express pathogenic ataxin-3, both “Intact” and “HNHH” live a lifespan that is markedly shorter (figure 2B). Control flies in this experiment contain the cloning vector (pWalium10-moe inserted at the attP2 site), without any ataxin-3 transgenes, and the sqh-Gal4 driver. Still, the “HNHH” mutation has a marked, early impact on the longevity of these flies when the transgene is expressed in all tissues of the fruit fly.

Next, we assessed by western blotting the expression of ataxin-3 protein in one-day-old, whole-fly lysates. Flies that harbor pathogenic ataxin-3 with intact VCP-binding show higher-molecular weight species, indicative of ataxin-3 SDS-resistant aggregates as early as one day after eclosion, whereas flies with mutated VCP-binding do not show this (figure 2C). In figure 2C and throughout the rest of this work, you will observe several ataxin-3-positive bands in western blots. The band highlighted as SDS-soluble species contains the unmodified version of this protein (bottom-most band) and what could be a phosphorylated form of ataxin-3 (immediately above it in lighter exposures in some instances; this band is not always visible; Fei et al., 2007; Kristensen et al., 2017; Matos et al., 2016). The asterisks denote ubiquitinated species of ataxin-3 (Todi et al., 2010; Todi et al., 2009; Tsou et al., 2013). The dotted line separates what we know are unmodified and ubiquitinated species of ataxin-3 from the higher-molecular weight species. The smear above the dotted line is consistent with SDS-resistant ataxin-3 species, based on our earlier work with this protein (Blount et al., 2014; Scaglione et al., 2011;

Sutton et al., 2017; Todi et al., 2009; Tsou et al., 2013; Tsou et al., 2015). In our extensive work with ataxin-3 *in vitro*, in mammalian cells, in *Drosophila* and in mouse models of this disease, we are confident that our delineation by the dotted line is a reasonable classification of ataxin-3 species that are SDS-soluble vs. not. The SDS-resistant species may contain higher-order aggregates of the SCA3 protein.

While aging the flies in the longevity experiment, we collected adults for western blot analysis after eclosion on days 1, 7 and 14 to examine the state of SDS-resistant and SDS-soluble species as flies age (figure 2D). As in figure 2C, SDS-resistant species are already clearly present on day 1 in flies that express the “Intact” pathogenic protein. This is significantly reduced in flies expressing the “HNHH” mutant form, and we do not observe comparable accumulation of SDS-resistant protein species until day 7 (figure 2D). Both “Intact” and "HNHH" flies show SDS-resistant species with age, but this accumulation is delayed in the “HNHH” flies.

To further examine the accumulation of aggregated species of pathogenic ataxin-3, we utilized differential centrifugation to separate whole fly lysates into a soluble, supernatant fraction and an insoluble, pellet fraction (figure 2E; Kim et al., 2011; O'Rourke et al., 2013; Santarriaga et al., 2015; Yang et al., 2014). As in prior blots, we quantified SDS-resistant smears and compared them to the total ataxin-3 signal in each lane. This analysis revealed a trend similar to previous panels: flies expressing ataxin-3 with mutated VCP-binding contain fewer SDS-resistant species early on. Their accumulation over time is delayed when compared to flies expressing ataxin-3 with intact VCP-binding (figure 2E).

Altogether, these experiments indicate that when the VCP-binding site of pathogenic ataxin-3 is mutated, there is a delay in the accumulation of aggregated protein species in flies, compared with their “Intact” counterparts. Disrupting the interaction between pathogenic ataxin-3 and VCP leads to markedly lower toxicity from pathogenic ataxin-3 during development and early on in the life of adult flies. These results prompted us to next explore the physiological impact of this mutation on the nervous system, the primary site of pathology in SCA3.

Pathogenic ataxin-3 with mutated VCP-binding is less toxic in fly neurons

Ataxin-3 is expressed in all tissues in the human body. However, SCA3 manifests with degeneration in specific areas, including the brainstem and the cerebellum (Costa Mdo and Paulson, 2012). We can direct the expression of pathogenic ataxin-3 only in the nervous system using a neuronal-specific driver, elav-Gal4, and examine its effects in the fly. Western blot analysis from one-day-old whole-fly lysates where pathogenic ataxin-3 with an intact VCP-binding site is expressed pan-neuronally shows the presence of SDS-resistant ataxin-3 in day one adults (figure 3A). Comparing the impaired VCP-binding flies to those expressing the “Intact” protein, the high molecular weight smear is significantly reduced (figure 3A; also see figure 3C, day 1). The control flies used in this experiment were ones containing the “Intact” pathogenic ataxin-3 transgene without the pan-neuronal driver; thus, there was no ataxin-3 expression in these flies.

Next, we aged adults to investigate how ataxin-3 expression in the nervous system affects their lifespan. Similarly to results with the ubiquitous driver (figure 2B), pan-neuronal expression of the VCP-binding site mutant delays lethality in adults compared

to the “Intact” form (figure 3B). However, even though in earlier time points more mutant “HNHH” flies remain alive, both fly lines have an average life span of 45 to 50 days (figure 3B). Flies expressing either variant of pathogenic ataxin-3 pan-neuronally live longer than those expressing the same constructs ubiquitously. This difference in toxicity is likely due to expression in all tissues of the fly, compared to only in the nervous system.

We examined by western blotting whole fly lysates at three points: day 1, day 7, and day 14 (figure 3C). Consistent with the results from ubiquitous expression (figure 2D), accumulation of SDS-resistant species is delayed when pathogenic ataxin-3 has a mutated VCP-binding site (figure 3C). You will note that the loading order for figure 3C is different from 2D. In 3C, we grouped samples by genotype, whereas in 2D we grouped them by day. We reasoned that it would be helpful to highlight the time-dependent effect of the VCP-binding site on ataxin-3 by organizing samples in these two different ways.

Because SCA3 is a movement disorder, we examined fly motility. We assessed how many flies reach the top of the vial within 5, 15 and 30 seconds on a weekly basis (figure 4). As early as day seven, flies expressing the “Intact” pathogenic protein are slower than control flies containing the empty vector across all three time points, and this difference increases markedly with age. Conversely, flies expressing pathogenic ataxin-3 with a mutated VCP-binding site perform as well as controls for up to three weeks (figure 4). We did not notice statistically significant reduction in the motility of these flies early on, a testament to the reduced toxicity of this protein in neurons, compared to the “Intact” counterparts. Finally, at four weeks of age, the “HNHH” flies also show slower motility compared to non-ataxin-3-expressing controls, but still perform

markedly better than flies expressing pathogenic ataxin-3 with intact VCP-binding (figure 4).

In conclusion, when the VCP-binding site of ataxin-3 is mutated, accumulation of SDS-resistant species in neurons is delayed and overall fly performance is improved.

Ataxin-3 with a mutated VCP-binding site is less toxic in Drosophila eyes

Drosophila eyes serve as a widely accepted model to study degeneration in various proteotoxic disorders (Bonini and Fortini, 2003; Kim et al., 2017). Histological sections of the fly eye allow visualization of degeneration and accumulation of proteinaceous aggregates. Using the GMR-Gal4 driver, we expressed the ataxin-3(SCA3) transgenes in fly eyes and conducted histological assays at different time points to characterize degeneration caused by expression of “Intact” pathogenic ataxin-3 and the effects of mutating its VCP-binding site on the phenotype.

The ommatidium is the functional unit of the fly eye. Each eye contains approximately 800 ommatidia arranged in a structured array. The highly iterative structure of the eye makes it a good model to easily and reliably observe perturbations arising from toxicity (Bonini and Fortini, 2003). Histological sections from one-week-old flies expressing pathogenic ataxin-3 with intact VCP-binding show that there is already some disruption of the internal ommatidial array of the eye (red bracketed lines) compared to the control flies, which did not express any pathogenic ataxin-3 (figure 5A, panel II compared to panel I). By comparison, eyes expressing the “HNHH” version of pathogenic ataxin-3 closely resemble control eyes, with a well-arranged ommatidial array and no clear signs of degeneration (figure 5A, panels III and IV). As SCA3 is a progressive dis-

ease, we expected to observe more degeneration as flies aged over the course of four weeks. This is the case for four-week-old fly eyes expressing the “Intact” pathogenic ataxin-3 protein, where we see an essentially obliterated internal eye (figure 5A, panel II). We also observe densely-staining structures, indicative of protein aggregates (red boxes; Warrick et al., 2005; Warrick et al., 1998). In "HNHH" eyes, we also begin to observe degeneration and some densely-staining structures (figure 5A, panels III and IV). Still, the ommatidia are present and largely well arrayed. We coupled histological assays with western blotting from dissected fly heads. Western blots from one-day-old fly heads show the presence of ataxin-3 SDS-resistant species, which is significantly reduced in the “HNHH” flies compared to the “Intact” flies (figure 5B).

We conclude that mutating the VCP-binding site of pathogenic ataxin-3 delays the formation of SDS-resistant species and slows the degeneration of fly eyes, similar to what we observe when these ataxin-3 forms are expressed in other tissues.

Knockdown of VCP improves degeneration caused by pathogenic ataxin-3

The above results indicate that pathogenic ataxin-3 protein is less toxic when its VCP-binding site is mutated. We wanted to confirm these differences in phenotype by targeting VCP itself. VCP is an essential protein with numerous functions in the cell. Knockdown of VCP in the whole fly, or in the nervous system, is developmentally lethal, but knockdown of VCP in fly eyes is tolerated (our own, unpublished observations). Thus, we examined whether knockdown of VCP in fly eyes expressing pathogenic ataxin-3 with intact VCP-binding impacts the structure of the eye.

From histological sections at four weeks of age, as shown above (figure 5A), expression of “Intact” pathogenic ataxin-3 in the eyes is toxic and causes the breakdown of the ommatidial array (figure 6A). We used two different RNAi lines targeting fly VCP. As shown in figure 6B, knockdown of VCP by each line leads to statistically significant reduction in VCP protein levels in the fly head. An important note here is that the blots underestimate the extent of VCP reduction; we target RNAi to the *Drosophila* eyes, but, unable to isolate only the eyes, we examine protein levels from whole fly heads, as is customary in fly studies.

Knockdown of VCP in fly eyes leads to improvement of pathology caused by ataxin-3. As shown in figure 6A, knocking down VCP with either RNAi-1 or -2 reduces ommatidial disarray in the presence of pathogenic ataxin-3. VCP RNAi-1 is not as effective as RNAi-2 at suppressing the degenerative phenotype. This could be due to the extent of VCP knockdown. RNAi-1 targeting VCP provides a somewhat larger reduction of VCP protein than RNAi-2, based on western blots (figure 6B). There may be a fine line between beneficial knockdown of VCP to suppress ataxin-3-dependent pathology and too much suppression, which might be problematic to the eye since we are targeting a crucial gene. RNAi-1 might be achieving this level of some improved pathology but also toxicity due to low VCP levels. Nevertheless, both RNAi lines present with improved pathology compared to pathogenic ataxin-3 with intact VCP-binding in the absence of RNAi. Concomitant with this improvement, we observe reduced levels of SDS-resistant species of ataxin-3 when VCP is knocked down (figure 6C).

In figure 6C, and to a lesser extent in earlier figures, a higher proportion of SDS-soluble ataxin-3 seems to be ubiquitinated in flies when VCP is knocked down or the

VCP-binding site is mutated. It is possible that when ataxin-3 proteins bind to VCP they are brought in close proximity and deubiquitinate each other. In conclusion, we observe decreased toxicity from ataxin-3 when VCP is knocked down in fly eyes, indicating that VCP enhances ataxin-3 aggregation and toxicity.

Correlating ataxin-3 SDS-resistant species to fly longevity

Our results with ubiquitous and pan-neuronal drivers show the presence of SDS-resistant ataxin-3 species with the “Intact” and “HNHH” versions before we observe marked lethality. We sought to further examine the temporal relationship between the SDS-resistant species and death. In our previous experiments, expression of pathogenic ataxin-3 was driven throughout development and adulthood. In the next round of studies, we induced ataxin-3 expression after adult fly eclosion and for specific points of time to examine the correlation between fly death and the accumulation of SDS-resistant ataxin-3 species.

We used the tissue-specific, inducible GeneSwitch Gal4 (Nicholson et al., 2008; Osterwalder et al., 2001; Roman and Davis, 2002; Sujkowski et al., 2015). Using this system, the pan-neuronal driver, elav-Gal4(GS) does not yield expression of ataxin-3 constructs until flies are fed RU-486, the compound which activates the driver. We raised flies that harbor the driver and ataxin-3 constructs in fly media without RU-486 and then switched them to RU-486-containing food on day 1 as adults. Offspring were then aged on RU-486-containing media and collected for western blotting on days 1, 4, 7, 10, 14, 21, 28 and 35. During this time, we also examined their longevity.

When pathogenic ataxin-3 with mutated VCP-binding is driven by RU-486 elav-Gal4(GS), we observe the appearance of SDS-resistant species later than with “Intact”. These smears increase in intensity over time for both the ataxin-3 “Intact” and “HNHH” (figure 7A). When the samples are compared side-by-side, on the same PVDF membrane, the difference in the timing of appearance of SDS-resistant species between the two forms of ataxin-3 is clear (figure 7B).

Based on longevity curves (figure 7C), temporally induced expression of pathogenic ataxin-3 with impaired VCP-binding leads to lethality later than “Intact”, correlating with delayed appearance of SDS-resistant species with “HNHH”. These results support our data from various tissues that the “HNHH” mutation delays the appearance of higher-molecular weight, SDS-resistant, ataxin-3-positive species in western blots, as well as the toxicity of this protein, compared to the “Intact” version.

SDS-resistant species of pathogenic ataxin-3 are stable once formed

Lastly, we utilized the RU-486-dependent elav-Gal4(GS) driver to examine the stability of the SDS-resistant species of pathogenic ataxin-3 *in vivo*. We wondered if eliminating the production of additional ataxin-3 leads to time-dependent dissipation of the SDS-resistant species, and if mutating its VCP-binding site influences this process. Ataxin-3 is a stable protein in the cellular environment (Todi et al., 2007a). Thus, we chased ataxin-3 for 21 days after we stopped its production by removing RU-486 from the fly media. To begin with comparable levels of the SDS-resistant species, we induced pathogenic ataxin-3 with an intact VCP-binding site for 7 days and the “HNHH” mutant form for 10 days in adult flies, based on results from figure 7B. Flies were raised in media

without RU-486 until eclosion. They were switched to media with the inducer on day 1 as adults (figure 8A). As shown in figure 8B, the SDS-resistant species are highly stable for the 21 days that we conducted our chases for both pathogenic ataxin-3 species. In fact, the intensity of the SDS-resistant species increases over time.

We tested if the physiological phenotypes of “Intact” and "HNHH" flies differ when the aggregated species begin at comparable levels, following the same parameters as above. In motility assays post-chase, there are no consistent, statistically significant differences between the performance of flies expressing either version of pathogenic ataxin-3 for the pre-determined time points we tested (figure 8C). These points were selected based on earlier data in this report and other studies with ataxin-3 (e.g. Sutton et al., 2017). When we monitor the longevity of these flies post-chase, HNHH-expressing flies overall live longer than ones with the “Intact” version of the SCA3 protein (figure 8D). In a variation of this experiment, we increased the induction of “Intact and “HNHH” ataxin-3 expression to 14 and 21 days, respectively. We collected results similar to figure 8 for each modality examined, again attesting to the stability of the SDS-resistant species of pathogenic ataxin-3, independently of the length of induction, and independently of the status of its VCP-binding site (figure 9).

Our interpretation of the results from figures 8 and 9 is that once SDS-resistant species of ataxin-3 are formed, they are highly stable. These data, combined with earlier figures (e.g. figures 2, 3 and 4) suggest that phenotypes for the “Intact” and “HNHH” flies are dependent on the different amounts of aggregated species. The difference in phenotype between the longevity and motility assays highlights the importance of using different assessments to understand outcomes from toxic proteins. The ability of HNHH-

expressing flies to live longer once expression of ataxin-3 is halted likely stems from reduced aggregative propensity of existing, soluble ataxin-3 when it cannot bind VCP (e.g. figure 8B). Still, the main point of the observations in figures 8 and 9 is that once formed, SDS-resistant ataxin-3 species are highly stable, can continue to accumulate, and the ability of ataxin-3 to bind to VCP does not seem important in their dissipation over time.

DISCUSSION

We tackled the interaction of the SCA3 protein, ataxin-3, with its direct binding protein, VCP, and the effect of this interaction in *Drosophila*. Ataxin-3 was reported previously to function with VCP to regulate degradation of ERAD substrates (Wang et al., 2006; Zhong and Pittman, 2006). Interestingly, while ataxin-3 has been ascribed various roles in cell culture-based studies, different knockout mouse lines that targeted the *atxn3* gene failed to show that this protein is a necessary entity in an intact mammal (Schmitt et al., 2007; Switonski et al., 2011). Based on knockout lines, we hypothesized some time ago that targeting the ataxin-3 protein to enhance its degradation might have therapeutic benefits. In those studies, we found that the VCP-ataxin-3 interaction did not impact the levels or turnover rate of ataxin-3 degradation (Blount et al., 2014). We also found that the VCP-binding capability of ataxin-3 was dispensable for its role in the fly, where it serves a neuroprotective role (Tsou et al., 2015).

The VCP-ataxin-3 interaction was described in detail by the Wanker and Bonini groups over a decade ago (Boeddrich et al., 2006). From that study, a model emerged where binding of multiple ataxin-3 proteins by a single VCP hexamer brings SCA3 proteins in close physical contact, nucleating early steps of their fibrillization. Intrigued by that work and by our own findings that the VCP-ataxin-3 interaction does not affect the degradation of ataxin-3 or its function in the fly, we investigated how this binding impacts ataxin-3 aggregation and toxicity *in vivo*. We found that accumulation of SDS-resistant species and insoluble aggregates occurs faster in flies expressing pathogenic ataxin-3 with intact VCP-binding than in flies expressing pathogenic ataxin-3 with mutated VCP-binding. The SDS-resistant species that we observe in western blots likely

consist of lower- and higher-order multimeric species of pathogenic ataxin-3. The insoluble pellet fractions we obtained from differential centrifugation may contain higher-order ataxin-3 multimers and oligomers (O'Rourke et al., 2013). Coincident with a delay in pathogenic ataxin-3 aggregation when its VCP-binding site is mutated (or when VCP is knocked down), we noticed reduced toxicity from this version of the SCA3 protein, compared to the “Intact” form. In each of our studies, ataxin-3 with impaired VCP-binding was less toxic in flies. In fact, at early stages, fly motility was entirely non-impacted by pathogenic ataxin-3 with impaired VCP-binding. Later on, these flies performed poorly when compared to flies not expressing the SCA3 protein, but still markedly better than the “Intact” flies. Thus, while interrupting the interaction between ataxin-3 and VCP had an early, ameliorative effect, in later stages the disease protein still proved toxic. This is an important finding, as it suggests that VCP enhances, but does not play a vital role, in the overall toxicity of the SCA3 protein. Also, from a therapeutic point of view, interrupting the interaction of ataxin-3 with VCP might have beneficial effects, but perhaps would not reach “curative” properties.

Collectively, our studies support a role for VCP in the early stages of ataxin-3 aggregation, consistent with a nucleation role for the hexamer put forth from *in vitro* work (Boeddrich et al., 2006; figure 9E). Non-pathogenic ataxin-3 itself has a propensity to aggregate. This is believed to happen through a two-step process based on work with recombinant proteins (Ellisdon et al., 2006; Masino et al., 2011; Masino et al., 2004). Wild-type ataxin-3 with a normal polyQ tract is thought to first dimerize through the catalytic, Josephin Domain in the structured N-terminus. In a second, less understood step, the C-terminal tails of the proteins come together to create a ‘bead-on-a-string’-type

structure, and these further assemble into SDS-soluble protein aggregates (Ellisdon et al., 2006; Masino et al., 2011). This process is thought to occur in the same two-step manner when ataxin-3 contains an expanded, pathogenic-range polyQ, although in that instance highly stable, SDS-resistant aggregates form *in vitro* (Ellisdon et al., 2006; Masino et al., 2011). We propose that VCP acts as a nucleating agent in initial ataxin-3 fibrillization. Ataxin-3 directly binds to VCP through its VCP-binding site. A VCP hexamer could bind multiple ataxin-3 proteins (Boeddrich et al., 2006). VCP hexamers, by binding to ataxin-3, increase the local concentration of the protein and also increase the likelihood of binding between ataxin-3 molecules and eventual formation into larger aggregates (figure 9E). Inhibiting this interaction, or reducing levels of VCP available for this step, decreases aggregation and ensuing toxicity.

A recent study by the Loll lab contradicts the model presented above. Utilizing wild-type, non-pathogenic ataxin-3 and VCP proteins produced in bacteria, their *in vitro* biochemical and electron microscopy work indicated that each VCP hexamer is bound by a single, wild type ataxin-3 (Rao et al., 2017). Work by Wanker and Bonini hinted at a stoichiometry of 4:1 ataxin-3:VCP (Boeddrich et al., 2006). Our own data in *Drosophila* are consistent with a stoichiometry different than 1:1. It could be that the VCP:ataxin-3 stoichiometry is 1:1 for wild type ataxin-3, but different for pathogenic ataxin-3. Also, unlike in an isolated system, it is possible that additional factors impact the stoichiometry between these two proteins *in vivo*. This is an area that requires additional investigation *in vivo*.

In summary, the VCP-binding site of ataxin-3 has a significant role on the aggregation and toxicity of the SCA3 protein *in vivo*, underscoring the importance of non-

polyQ domains in this disease and pointing to the ataxin-3-VCP interaction as a potential therapeutic target. The model for VCP hexamer-mediated aggregation may extend beyond SCA3, since VCP also interacts with other polyQ proteins (Fujita et al., 2013).

ACKNOWLEDGEMENTS

We thank Ms. Jessica R. Blount for her help with mutagenesis and cloning of the Ataxin-3(SCA3)-HNHH construct.

FUNDING

This work was funded by a Wayne State University Thomas Rumble Fellowship to GR, by an F31 fellowship to JRS from NINDS (F31NS095575), by a Pilot Grant Award from the Department of Pharmacology at Wayne State University to SVT, by R01NS038712 and by R01NS086778 to SVT from NINDS.

DECLARATIONS OF INTEREST: The authors do not have anything to declare.

REFERENCES

Albrecht, M., Golatta, M., Wullner, U., and Lengauer, T. (2004). Structural and functional analysis of ataxin-2 and ataxin-3. Eur J Biochem *271*, 3155-3170.

Blount, J.R., Tsou, W.L., Ristic, G., Burr, A.A., Ouyang, M., Galante, H., Scaglione, K.M., and Todi, S.V. (2014). Ubiquitin-binding site 2 of ataxin-3 prevents its proteasomal degradation by interacting with Rad23. Nat Commun *5*, 4638.

Boeddrich, A., Gaumer, S., Haacke, A., Tzvetkov, N., Albrecht, M., Evert, B.O., Muller, E.C., Lurz, R., Breuer, P., Schugardt, N.*, et al.* (2006). An arginine/lysine-rich motif is crucial for VCP/p97-mediated modulation of ataxin-3 fibrillogenesis. Embo J *25*, 1547-1558.

Bonini, N.M., and Fortini, M.E. (2003). Human neurodegenerative disease modeling using Drosophila. Annu Rev Neurosci *26*, 627-656.

Brand, A.H., Manoukian, A.S., and Perrimon, N. (1994). Ectopic expression in Drosophila. Methods Cell Biol *44*, 635-654.

Brand, A.H., and Perrimon, N. (1993). Targeted gene expression as a means of altering cell fates and generating dominant phenotypes. Development *118*, 401-415.

Costa Mdo, C., and Paulson, H.L. (2012). Toward understanding Machado-Joseph disease. Prog Neurobiol *97*, 239-257.

Doss-Pepe, E.W., Stenroos, E.S., Johnson, W.G., and Madura, K. (2003). Ataxin-3 interactions with rad23 and valosin-containing protein and its associations with ubiquitin chains and the proteasome are consistent with a role in ubiquitin-mediated proteolysis. Mol Cell Biol *23*, 6469-6483.

Ellisdon, A.M., Thomas, B., and Bottomley, S.P. (2006). The two-stage pathway of ataxin-3 fibrillogenesis involves a polyglutamine-independent step. J Biol Chem *281*, 16888-16896.

Fei, E., Jia, N., Zhang, T., Ma, X., Wang, H., Liu, C., Zhang, W., Ding, L., Nukina, N., and Wang, G. (2007). Phosphorylation of ataxin-3 by glycogen synthase kinase 3beta at serine 256 regulates the aggregation of ataxin-3. Biochem Biophys Res Commun *357*, 487-492.

Fujita, K., Nakamura, Y., Oka, T., Ito, H., Tamura, T., Tagawa, K., Sasabe, T., Katsuta, A., Motoki, K., Shiwaku, H.*, et al.* (2013). A functional deficiency of TERA/VCP/p97 contributes to impaired DNA repair in multiple polyglutamine diseases. Nat Commun *4*, 1816.

Groth, A.C., Fish, M., Nusse, R., and Calos, M.P. (2004). Construction of transgenic Drosophila by using the site-specific integrase from phage phiC31. Genetics *166*, 1775-1782.

Hirabayashi, M., Inoue, K., Tanaka, K., Nakadate, K., Ohsawa, Y., Kamei, Y., Popiel, A.H., Sinohara, A., Iwamatsu, A., Kimura, Y.*, et al.* (2001). VCP/p97 in abnormal protein aggregates, cytoplasmic vacuoles, and cell death, phenotypes relevant to neurodegeneration. Cell Death Differ *8*, 977-984.

Kim, S.H., Stiles, S.G., Feichtmeier, J.M., Ramesh, N., Zhan, L., Scalf, M.A., Smith, L.M., Pandey, U.B., and Tibbetts, R.S. (2017). Mutation-dependent aggregation and toxicity in a Drosophila model for UBQLN2-associated ALS. Hum Mol Genet.

Kim, Y.M., Jang, W.H., Quezado, M.M., Oh, Y., Chung, K.C., Junn, E., and Mouradian, M.M. (2011). Proteasome inhibition induces alpha-synuclein SUMOylation and aggregate formation. J Neurol Sci *307*, 157-161.

Kristensen, L.V., Oppermann, F.S., Rauen, M.J., Hartmann-Petersen, R., and Thirstrup, K. (2017). Polyglutamine expansion of ataxin-3 alters its degree of ubiquitination and phosphorylation at specific sites. Neurochem Int *105*, 42-50.

Masino, L., Nicastro, G., De Simone, A., Calder, L., Molloy, J., and Pastore, A. (2011). The Josephin domain determines the morphological and mechanical properties of ataxin-3 fibrils. Biophys J *100*, 2033-2042.

Masino, L., Nicastro, G., Menon, R.P., Dal Piaz, F., Calder, L., and Pastore, A. (2004). Characterization of the structure and the amyloidogenic properties of the Josephin domain of the polyglutamine-containing protein ataxin-3. J Mol Biol *344*, 1021-1035.

Matos, C.A., de Macedo-Ribeiro, S., and Carvalho, A.L. (2011). Polyglutamine diseases: The special case of ataxin-3 and Machado-Joseph disease. Prog Neurobiol *95*, 26-48.

Matos, C.A., Nobrega, C., Louros, S.R., Almeida, B., Ferreiro, E., Valero, J., Pereira de Almeida, L., Macedo-Ribeiro, S., and Carvalho, A.L. (2016). Ataxin-3 phosphorylation decreases neuronal defects in spinocerebellar ataxia type 3 models. J Cell Biol *212*, 465-480.

Meyer, H., Bug, M., and Bremer, S. (2012). Emerging functions of the VCP/p97 AAA-ATPase in the ubiquitin system. Nat Cell Biol *14*, 117-123.

Nicholson, L., Singh, G.K., Osterwalder, T., Roman, G.W., Davis, R.L., and Keshishian, H. (2008). Spatial and temporal control of gene expression in Drosophila using the inducible GeneSwitch GAL4 system. I. Screen for larval nervous system drivers. Genetics *178*, 215-234.

O'Rourke, J.G., Gareau, J.R., Ochaba, J., Song, W., Rasko, T., Reverter, D., Lee, J., Monteys, A.M., Pallos, J., Mee, L.*, et al.* (2013). SUMO-2 and PIAS1 modulate insoluble mutant huntingtin protein accumulation. Cell Rep *4*, 362-375.

Osterwalder, T., Yoon, K.S., White, B.H., and Keshishian, H. (2001). A conditional tissue-specific transgene expression system using inducible GAL4. Proc Natl Acad Sci U S A *98*, 12596-12601.

Paulson, H.L., Das, S.S., Crino, P.B., Perez, M.K., Patel, S.C., Gotsdiner, D., Fischbeck, K.H., and Pittman, R.N. (1997). Machado-Joseph disease gene product is a cytoplasmic protein widely expressed in brain. Ann Neurol *41*, 453-462.

Rao, M.V., Williams, D.R., Cocklin, S., and Loll, P.J. (2017). Interaction between the AAA(+) ATPase p97 and its cofactor ataxin3 in health and disease: Nucleotide-induced conformational changes regulate cofactor binding. J Biol Chem *292*, 18392-18407.

Reina, C.P., Nabet, B.Y., Young, P.D., and Pittman, R.N. (2012). Basal and stress-induced Hsp70 are modulated by ataxin-3. Cell Stress Chaperones.

Roman, G., and Davis, R.L. (2002). Conditional expression of UAS-transgenes in the adult eye with a new gene-switch vector system. Genesis *34*, 127-131.

Santarriaga, S., Petersen, A., Ndukwe, K., Brandt, A., Gerges, N., Bruns Scaglione, J., and Scaglione, K.M. (2015). The Social Amoeba Dictyostelium discoideum Is Highly Resistant to Polyglutamine Aggregation. J Biol Chem *290*, 25571-25578.

Scaglione, K.M., Zavodszky, E., Todi, S.V., Patury, S., Xu, P., Rodriguez-Lebron, E., Fischer, S., Konen, J., Djarmati, A., Peng, J.*, et al.* (2011). Ube2w and Ataxin-3 Coordinately Regulate the Ubiquitin Ligase CHIP. Mol Cell *43*, 599-612.

Schmitt, I., Linden, M., Khazneh, H., Evert, B.O., Breuer, P., Klockgether, T., and Wuellner, U. (2007). Inactivation of the mouse Atxn3 (ataxin-3) gene increases protein ubiquitination. Biochem Biophys Res Commun *362*, 734-739.

Sujkowski, A., Bazzell, B., Carpenter, K., Arking, R., and Wessells, R.J. (2015). Endurance exercise and selective breeding for longevity extend Drosophila healthspan by overlapping mechanisms. Aging (Albany NY) *7*, 535-552.

Sutton, J.R., Blount, J.R., Libohova, K., Tsou, W.L., Joshi, G.S., Paulson, H.L., Costa, M.D.C., Scaglione, K.M., and Todi, S.V. (2017). Interaction of the polyglutamine protein ataxin-3 with Rad23 regulates toxicity in Drosophila models of Spinocerebellar Ataxia Type 3. Hum Mol Genet *26*, 1419-1431.

Switonski, P.M., Fiszer, A., Kazmierska, K., Kurpisz, M., Krzyzosiak, W.J., and Figiel, M. (2011). Mouse ataxin-3 functional knock-out model. Neuromolecular Med *13*, 54-65.

Todi, S.V., Laco, M.N., Winborn, B.J., Travis, S.M., Wen, H.M., and Paulson, H.L. (2007a). Cellular turnover of the polyglutamine disease protein ataxin-3 is regulated by its catalytic activity. J Biol Chem *282*, 29348-29358.

Todi, S.V., Scaglione, K.M., Blount, J.R., Basrur, V., Conlon, K.P., Pastore, A., Elenitoba-Johnson, K., and Paulson, H.L. (2010). Activity and cellular functions of the deubiquitinating enzyme and polyglutamine disease protein ataxin-3 are regulated by ubiquitination at lysine 117. J Biol Chem *285*, 39303-39313.

Todi, S.V., Williams, A., and Paulson, H. (2007b). Polyglutamine Repeat Disorders, including Huntington's Disease. In Molecular Neurology, S.G. Waxman, ed. (London: Academic Press), pp. 257-276.

Todi, S.V., Winborn, B.J., Scaglione, K.M., Blount, J.R., Travis, S.M., and Paulson, H.L. (2009). Ubiquitination directly enhances activity of the deubiquitinating enzyme ataxin-3. EMBO J *28*, 372-382.

Tsou, W.L., Burr, A.A., Ouyang, M., Blount, J.R., Scaglione, K.M., and Todi, S.V. (2013). Ubiquitination regulates the neuroprotective function of the deubiquitinase ataxin-3 in vivo. J Biol Chem *288*, 34460-34469.

Tsou, W.L., Ouyang, M., Hosking, R.R., Sutton, J.R., Blount, J.R., Burr, A.A., and Todi, S.V. (2015). The deubiquitinase ataxin-3 requires Rad23 and DnaJ-1 for its neuroprotective role in Drosophila melanogaster. Neurobiol Dis *82*, 12-21.

Tsou, W.L., Qiblawi, S.H., Hosking, R.R., Gomez, C.M., and Todi, S.V. (2016). Polyglutamine length-dependent toxicity from alpha1ACT in Drosophila models of spinocerebellar ataxia type 6. Biol Open *5*, 1770-1775.

Wang, Q., Li, L., and Ye, Y. (2006). Regulation of retrotranslocation by p97-associated deubiquitinating enzyme ataxin-3. J Cell Biol *174*, 963-971.

Warrick, J.M., Morabito, L.M., Bilen, J., Gordesky-Gold, B., Faust, L.Z., Paulson, H.L., and Bonini, N.M. (2005). Ataxin-3 suppresses polyglutamine neurodegeneration in Drosophila by a ubiquitin-associated mechanism. Mol Cell *18*, 37-48.

Warrick, J.M., Paulson, H.L., Gray-Board, G.L., Bui, Q.T., Fischbeck, K.H., Pittman, R.N., and Bonini, N.M. (1998). Expanded polyglutamine protein forms nuclear inclusions and causes neural degeneration in Drosophila. Cell *93*, 939-949.

Xia, D., Tang, W.K., and Ye, Y. (2016). Structure and function of the AAA+ ATPase p97/Cdc48p. Gene *583*, 64-77.

Yang, H., Li, J.J., Liu, S., Zhao, J., Jiang, Y.J., Song, A.X., and Hu, H.Y. (2014). Aggregation of polyglutamine-expanded ataxin-3 sequesters its specific interacting partners into inclusions: implication in a loss-of-function pathology. Sci Rep *4*, 6410.

Zhong, X., and Pittman, R.N. (2006). Ataxin-3 binds VCP/p97 and regulates retrotranslocation of ERAD substrates. Hum Mol Genet *15*, 2409-2420.

FIGURE LEGENDS

Figure 1: Pathogenic ataxin-3 with a mutated VCP-binding site does not bind *Drosophila* VCP.

A) Diagrammatic representation of ataxin-3. The catalytic domain of ataxin-3, Josephin Domain, is located at the structured, N-terminal half of the protein. The inherently unstructured, C-terminal portion contains three Ubiquitin Interacting Motifs (UIMs), the polyQ tract (which is abnormally expanded in SCA3 patients), and the VCP-binding site. Box shows this site was mutated from “RKRR” to “HNHH” to disrupt its interaction with VCP. **B)** Diagrammatic representation of VCP. VCP functions as a homohexamer. Each VCP protein contains an N-terminal domain (through which it binds to most of its co-factors, including ataxin-3), two tandem ATPase domains, and a short C-terminal tail. **C)** Western blots from *in vitro* pull-downs with whole fly lysates and immobilized, recombinant GST, GST-Ataxin-3(SCA3)-Intact, or GST-Ataxin-3(SCA3)-HNHH. The ataxin-3(SCA3) constructs contain 80Q. Blots are representative of experiments repeated independently three times with the same outcomes. The VCP protein band appears at ~100kDa and the GST-tagged pathogenic ataxin-3 protein band appears at ~90kDa due to the size of the GST tag. Ataxin-3 with ~80 polyQ that is untagged or has FLAG or HA tags migrates at ~65kDa. **D)** Western blots of co-immunoprecipitations from HEK293 cells transiently transfected with the indicated constructs. Both Ataxin-3(SCA3) constructs contain 80Q. In this panel and the rest of the figures, pathogenic ataxin-3 migrates at about ~65kDa. Blots are representative of experiments repeated independently three times with the same outcomes. NS: Nonspecific band we often observe with the polyclonal ataxin-3 antibody. In panels E-G and the rest of the figures in this manuscript,

Ataxin-3(SCA3)-Intact contains 77Q. Ataxin-3(SCA3)-HNHH constructs contain 80Q. **E)** Western blots of co-immunoprecipitations from dissected heads of transgenic flies expressing the indicated constructs. Transgenes were expressed through the eye-specific, GMR-Gal4 driver. Blots are representative of experiments repeated independently at least three times with the same outcomes. In this panel and the rest of the figures, flies were heterozygous for all drivers and transgenes. **F)** qRT-PCR results from whole adult flies expressing pathogenic ataxin-3 with an intact or mutated VCP-binding site. Ataxin-3(SCA3)-Intact or Ataxin-3(SCA3)-HNHH was driven by the sqh-Gal4 ubiquitous driver. N=4 independent repeats. In this panel and the rest of the figures, HNHH-1 and -2 are independently-derived transgenic lines. Endogenous control: rp49. Histograms represent means ± SD, expressed as a percentage. No statistical differences were observed by Student *t*-tests comparing HNHH-1 or -2 to Intact. **G)** Western blots of fly lysates after cytoplasmic/nuclear centrifugal fractionation. Transgenic adult flies expressed pathogenic ataxin-3 with or without the VCP-binding site mutated from “RKRR” to “HNHH”. Ataxin-3(SCA3)-Intact or Ataxin-3(SCA3)-HNHH were expressed under the control of the sqh-Gal4 driver. “Intact Control” flies were Ataxin-3(SCA3)-Intact-containing flies without a driver. Asterisks: ubiquitinated ataxin-3. NS: Nonspecific band. Blots are representative of experiments repeated independently three times with the same outcomes.

Figure 2: Mutating the VCP-binding site of pathogenic ataxin-3 delays its aggregation and toxicity when expressed in all fly tissues.

In all panels, transgenes were expressed using the ubiquitous driver, sqh-Gal4. **A)** Summary of effects on fly development and longevity when pathogenic ataxin-3 with an intact or mutated VCP-binding site is expressed in all fly tissues. **B)** Longevity of adult flies ubiquitously expressing pathogenic ataxin-3 with or without the VCP-binding site mutated from RKRR to HNHH. Control flies contained the sqh-Gal4 driver and the empty host vector (pWalium10-moe) inserted at the attP2 site, without an ataxin-3 transgene. Control flies live up to ~90 days. **C, D)** Western blots from one-day-old flies (C) or flies of different ages (D) expressing pathogenic ataxin-3 with or without mutated VCP-binding site. Histograms represent means ± SD, expressed as a percentage. SDS-Resistant signal was quantified by measuring the signal above the dotted line and dividing it by the total ataxin-3 signal (SDS-Soluble + SDS-Resistant) in that same lane. This was performed for all histograms where we quantify SDS-resistant species of ataxin-3, throughout this work. Asterisks in histograms: $p<0.05$ from Student's *t*-tests comparing each HNHH line to the Intact line of the respective age group. N=5 independent repeats for panel C and N=3 independent repeats for panel D. In panels C-E and the rest of the figures in this manuscript, dotted lines help to visually categorize ataxin-3 species into SDS-soluble and SDS-resistant. Asterisks in blots in panels C, D, E: ubiquitinated ataxin-3. **E)** Western blot from differential centrifugation of fly lysates into soluble supernatant and insoluble pellet fractions. Ten µg of supernatant and 7 µL of pellet fractions were electrophoresed on 4-20% gradient gels. Histograms represent means ± SD, quantified as in panels C and D. Asterisks in histograms: $p<0.05$ from Student's *t*-tests,

comparing signal from each time point to the “Day 1-Soluble” point of each genotype. N=3 independent repeats.

Figure 3: Mutating the VCP-binding site of pathogenic ataxin-3 delays its aggregation and toxicity when expressed pan-neuronally.

In all panels, transgenes were expressed using the pan-neuronal, elav-Gal4 driver. **A, C)** Western blots from one-day-old flies (A) or flies of different ages (C) when pathogenic ataxin-3 with or without a mutation of its VCP-binding site is expressed in the nervous system. Control flies contained the Ataxin-3(SCA3)-Intact transgene, but without a Gal4 driver. NS: nonspecific band we observe sometimes with the monoclonal anti-ataxin-3 antibody when this transgene is expressed pan-neuronally; this band is immediately below SDS-soluble ataxin-3 in panel C. Histograms represent means ± SD, expressed as a percentage. Asterisks in histograms: $p<0.05$ from Student’s *t*-tests comparing each HNHH line to their age group Intact. N=6 independently conducted repeats for panel A and N=8 independent repeats for panel C. **B)** Longevity assay from adult *Drosophilae* pan-neuronally expressing pathogenic ataxin-3 with an intact or mutated VCP-binding site. Control flies contained the empty host vector in the presence of the elav-Gal4 driver.

Figure 4: Flies that express pathogenic ataxin-3 with a mutated VCP-binding site are indistinguishable from non-ataxin-3 flies early on in a motility assay.

Results from a negative geotaxis assay used to assess the motility of flies expressing pathogenic ataxin-3 with or without mutated VCP-binding. Ataxin-3 transgenes were ex-

pressed using the pan-neuronal elav-Gal4 driver. Histograms represent means ± SD, expressed as a percentage, of flies able to reach the top of the vial at the indicated time points. Asterisks in histograms: $p<0.05$, from Student's *t*-tests, comparing Ataxin-3(SCA3)-Intact and -HNHH to "No Ataxin-3". "No Ataxin-3" flies contained the elav-Gal4 driver and the empty host vector. N=5 independent repeats, totaling at least 100 flies per genotype.

Figure 5: Disrupting the interaction between ataxin-3 and VCP reduces toxicity in fly eyes.

In all panels, transgenes were expressed using the eye-specific, GMR-Gal4 driver. **A)** Histological sections of fly eyes expressing pathogenic ataxin-3 with or without mutated VCP-binding at one week or four weeks of age. "Vector Ctrl" flies contain the GMR-Gal4 driver and the empty host vector. Red boxes: examples of densely-staining structures. Red bracketed lines: ommatidial boundaries. Longer lines indicate loss of these boundaries. **B)** Western blots from lysates of fly heads dissected from one-day-old flies. Histograms represent means ± SD, expressed as a percentage. Asterisks in histograms: $p<0.05$ from Student's *t*-tests comparing each HNHH line to Intact. N=3 independent repeats.

Figure 6: Knockdown of VCP in fly eyes improves degeneration caused by pathogenic ataxin-3.

In all panels, transgenes were expressed using the eye-specific, GMR-Gal4 driver. **A)** Histological sections of four-week-old fly eyes expressing pathogenic ataxin-3 with or

without VCP RNAi. "Vector Ctrl" contained the GMR-Gal4 driver and empty host vector on the same genetic background as the RNAi lines. Red boxes: examples of densely-staining structures. Red bracketed lines: ommatidial boundaries. **B)** Quantification of VCP protein levels from panel C and other, independent repeats. Histograms represent means ± SD, expressed as a percentage. Asterisks in histograms: $p<0.05$ from Student's *t*-tests, comparing VCP RNAi-1 or 2 to the Control. N=6 independent repeats. **C)** Western blots of one-day-old fly head lysates when pathogenic ataxin-3 is expressed alone or alongside VCP RNAi in fly eyes. Red dotted line: portion of SDS-resistant ataxin-3 species most clearly diminished in intensity by the knockdown of VCP. Black dotted line was drawn consistent with the same line in blots from prior figures. Histograms represent means ± SD, expressed as a percentage. Asterisks in histograms: $p<0.05$ from Student's *t*-tests, comparing VCP RNAi-1 or -2 to Control. N=6 independent repeats. The signal quantified was from the dotted red line to the top of the membrane.

Figure 7: Correlation of ataxin-3 SDS-resistant species and longevity in flies.

In all panels, transgenes were expressed using the pan-neuronal, RU-486-inducible elav-Gal4(GS) driver. **A, B)** Western blots of fly lysates at the indicated days when pan-neuronal expression of pathogenic ataxin-3 with intact or mutated VCP-binding was induced immediately upon eclosion from the pupal case. NS: non-specific band. Histograms represent means ± SD, expressed as a percentage. Asterisks in histograms: $p<0.05$ from Student's *t*-tests comparing Intact or HNHH Days 7-35 to their respective Day 1. N=5 independent repeats. **C)** Longevity of flies when pan-neuronal expression of

pathogenic ataxin-3 with or without a mutation on the VCP-binding site is induced upon adult eclosion from the pupal case.

Figure 8: Ataxin-3 aggregates are stable, independently of VCP-binding.

In all panels, transgenes were expressed using the pan-neuronal, RU-486-inducible elav-Gal4(GS) driver. **A)** Outline of the experimental design for pulse-chases. Ataxin-3(SCA3)-Intact was induced for 7 days and -HNHH was induced for 10 days, each followed by a chase period. **B)** Western blots from whole fly lysates where pan-neuronal expression of pathogenic ataxin-3 with or without the VCP-binding mutation was induced and chased for the indicated time points. Histograms represent means ± SD, expressed as a percentage. Asterisks in histograms: $p<0.05$, from Student's *t*-tests, comparing Ataxin-3(SCA3)-Intact or -HNHH Days 1-21 to their respective Day 0. N=3 independent repeats. **C)** Results from negative geotaxis assays assessing the motility of flies when pathogenic ataxin-3 was induced and then chased for the indicated time points. Motility was assessed on Day 1, 21, and 28 of the flies' total adult lifespan. Histograms represent means ± SD, expressed as a percentage, of flies able to reach the top of the vial at the indicated time points. Asterisk in histogram: $p<0.05$, from Student's *t*-tests, comparing Ataxin-3(SCA3)-HNHH to -Intact. No other statistical significances were observed. At least 50 flies were assessed per genotype. **D)** Longevity of flies when pan-neuronal expression of pathogenic ataxin-3 without or with a mutation on the VCP-binding site is induced for 7 or 10 days, respectively, upon eclosion from the pupal case.

Figure 9: Longer induction of pathogenic ataxin-3 expression also yields highly stable aggregates.

In panels A-D, transgenes were expressed using the pan-neuronal, RU-486-inducible elav-Gal4(GS) driver. **A)** Outline of the experimental design for pulse-chases of pathogenic ataxin-3 with an intact or mutated VCP-binding site. Ataxin-3(SCA3)-Intact was induced for 14 days and Ataxin-3(SCA3)-HNHH was induced for 21 days, each followed by a chase period. **B)** Western blots from whole fly lysates where pan-neuronal expression of pathogenic ataxin-3 with or without the VCP-binding mutation was induced and chased for the indicated time points. Histograms represent means ± SD, expressed as a percentage. Student's *t*-tests yielded no statistically significant differences comparing Intact and HNHH signal from Days 7 and 14 to their respective Day 1. N=3 independent repeats. **C)** Results from negative geotaxis assays assessing the motility of flies when pathogenic ataxin-3 was induced and then chased for the indicated time points. Motility was assessed on Day 1, 21, and 28 of the flies' total adult lifespan. Histograms represent the means ± SD, expressed as a percentage, of flies able to reach the top of the vial at the indicated time points. Student's *t*-tests yielded no statistically significant differences comparing Ataxin-3(SCA3)-HNHH to -Intact. At least 50 flies were assessed per genotype. **D)** Longevity of flies when pan-neuronal expression of pathogenic ataxin-3 without or with a mutation of the VCP-binding site is induced for 14 or 21 days, respectively, upon eclosion from the pupal case. **E)** Model: Ataxin-3 directly binds to VCP through the VCP-binding site on its C-Terminal half. VCP hexamers act as nucleating agents and increase the local concentration of ataxin-3, leading to higher chances of interaction and aggregation of the SCA3 protein.

Highlights

- The causative protein in Spinocerebellar Ataxia Type 3, ataxin-3, binds VCP
- Polyglutamine expansion in ataxin-3 is toxic in *Drosophila melanogaster*
- This interaction regulates the aggregative propensity and toxicity of ataxin-3
- Inhibiting this interaction or reducing VCP levels decreases ataxin-3 toxicity in flies
- The direct interaction of ataxin-3 with VCP may be a good therapeutic target for SCA3

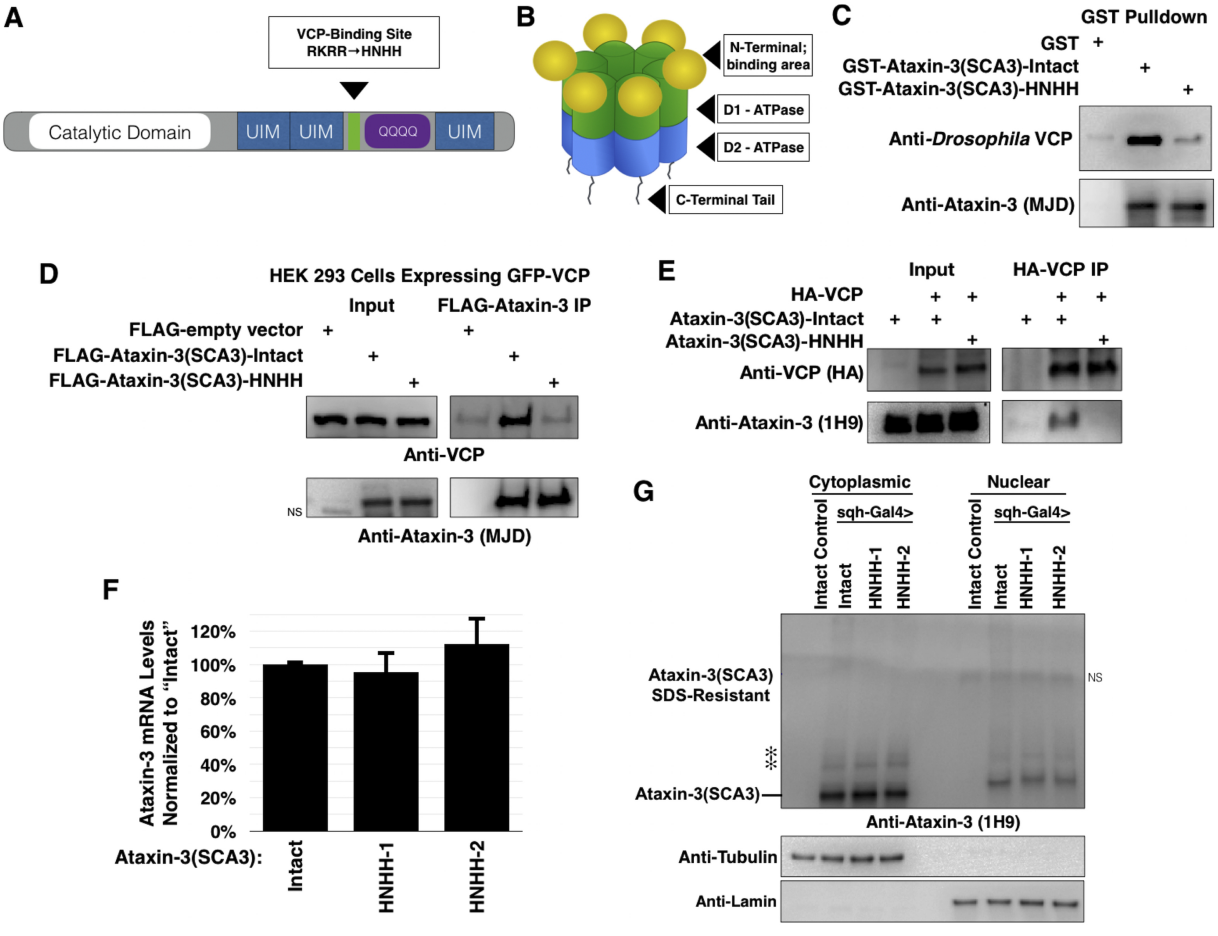
A
VCP-Binding Site
RKRR→HNHH
Catalytic Domain
UIM
UIM
QQQQ
UIM
B
N-Terminal; binding area
D1 - ATPase
D2 - ATPase
C-Terminal Tail
C
GST Pulldown
GST
GST-Ataxin-3(SCA3)-Intact
GST-Ataxin-3(SCA3)-HNHH
Anti-Drosophila VCP
Anti-Ataxin-3 (MJD)
D
HEK 293 Cells Expressing GFP-VCP
Input
FLAG-Ataxin-3 IP
FLAG-empty vector
FLAG-Ataxin-3(SCA3)-Intact
FLAG-Ataxin-3(SCA3)-HNHH
Anti-VCP
NS
Anti-Ataxin-3 (MJD)
E
Input
HA-VCP IP
HA-VCP
Ataxin-3(SCA3)-Intact
Ataxin-3(SCA3)-HNHH
Anti-VCP (HA)
Anti-Ataxin-3 (1H9)
F
Ataxin-3 mRNA Levels Normalized to "Intact"
120%
100%
80%
60%
40%
20%
0%
Ataxin-3(SCA3):
Intact
HNHH-1
HNHH-2
G
Cytoplasmic
Nuclear
Intact Control
sqh-Gal4>
Intact
HNHH-1
HNHH-2
Ataxin-3(SCA3) SDS-Resistant
Ataxin-3(SCA3)
NS
Anti-Ataxin-3 (1H9)
Anti-Tubulin
Anti-Lamin

Figure 1

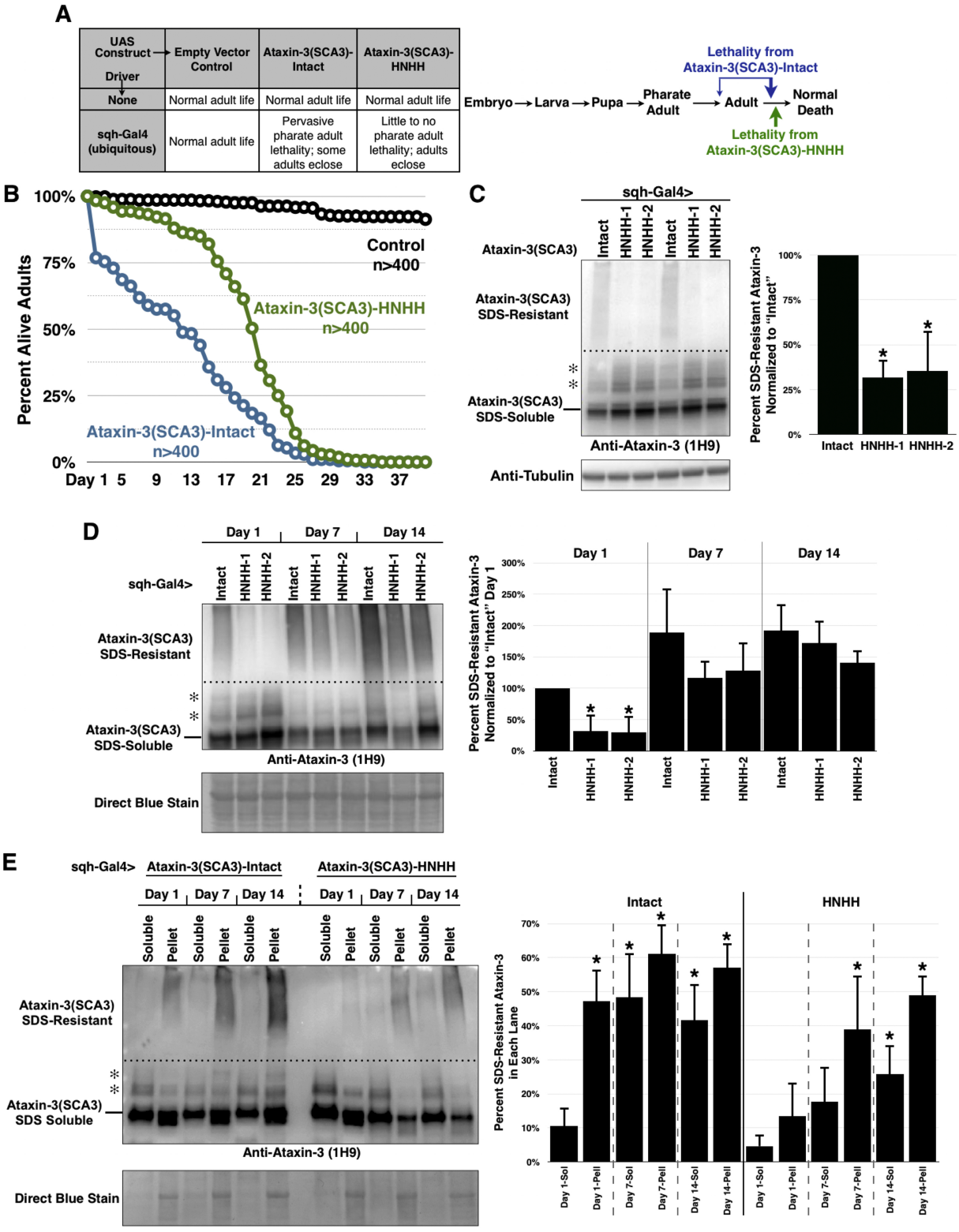
A
UAS Construct
Driver
Empty Vector Control
Ataxin-3(SCA3)-Intact
Ataxin-3(SCA3)-HNHH
None
Normal adult life
Normal adult life
Normal adult life
sqh-Gal4 (ubiquitous)
Normal adult life
Pervasive pharate adult lethality; some adults eclose
Little to no pharate adult lethality; adults eclose
Embryo → Larva → Pupa → Pharate Adult → Adult → Normal Death
Lethality from Ataxin-3(SCA3)-Intact
Lethality from Ataxin-3(SCA3)-HNHH
B
Percent Alive Adults
100%
75%
50%
25%
0%
Day 1 5 9 13 17 21 25 29 33 37
Control n>400
Ataxin-3(SCA3)-HNHH n>400
Ataxin-3(SCA3)-Intact n>400
C
sqh-Gal4>
Intact HNHH-1 HNHH-2 Intact HNHH-1 HNHH-2
Ataxin-3(SCA3)
Ataxin-3(SCA3) SDS-Resistant
Ataxin-3(SCA3) SDS-Soluble
Anti-Ataxin-3 (1H9)
Anti-Tubulin
Percent SDS-Resistant Ataxin-3 Normalized to "Intact"
Intact HNHH-1 HNHH-2
D
Day 1 Day 7 Day 14
sqh-Gal4>
Intact HNHH-1 HNHH-2 Intact HNHH-1 HNHH-2 Intact HNHH-1 HNHH-2
Ataxin-3(SCA3) SDS-Resistant
Ataxin-3(SCA3) SDS-Soluble
Anti-Ataxin-3 (1H9)
Direct Blue Stain
Percent SDS-Resistant Ataxin-3 Normalized to "Intact" Day 1
300% 250% 200% 150% 100% 50% 0%
Day 1 Day 7 Day 14
Intact HNHH-1 HNHH-2 Intact HNHH-1 HNHH-2 Intact HNHH-1 HNHH-2
E
sqh-Gal4> Ataxin-3(SCA3)-Intact Ataxin-3(SCA3)-HNHH
Day 1 Day 7 Day 14 Day 1 Day 7 Day 14
Soluble Pellet Soluble Pellet Soluble Pellet Soluble Pellet Soluble Pellet Soluble Pellet
Ataxin-3(SCA3) SDS-Resistant
Ataxin-3(SCA3) SDS Soluble
Anti-Ataxin-3 (1H9)
Direct Blue Stain
Percent SDS-Resistant Ataxin-3 in Each Lane
70% 60% 50% 40% 30% 20% 10% 0%
Intact
HNHH
Day 1-Sol Day 1-Pell Day 7-Sol Day 7-Pell Day 14-Sol Day 14-Pell Day 1-Sol Day 1-Pell Day 7-Sol Day 7-Pell Day 14-Sol Day 14-Pell

Figure 2

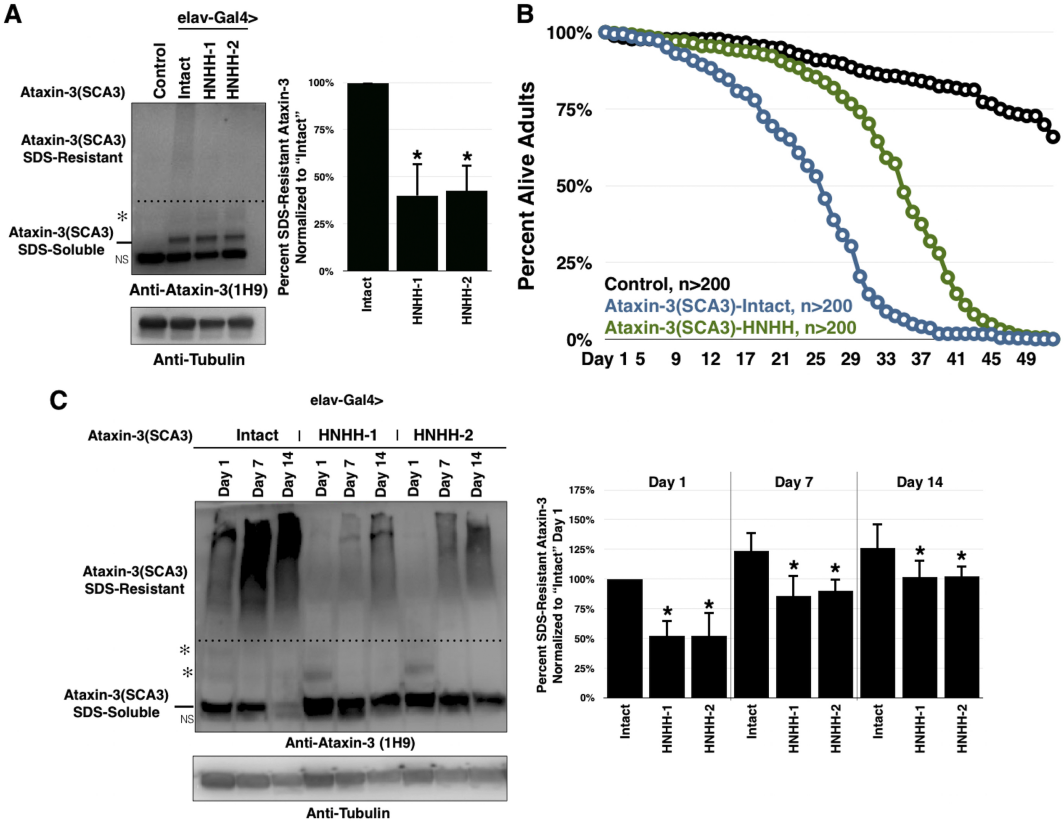
A
elav-Gal4>
Control
Intact
HNHH-1
HNHH-2
Ataxin-3(SCA3)
Ataxin-3(SCA3)
SDS-Resistant
Ataxin-3(SCA3)
SDS-Soluble
NS
Anti-Ataxin-3(1H9)
Anti-Tubulin
Percent SDS-Resistant Ataxin-3
Normalized to "Intact"
100%
75%
50%
25%
0%
Intact
HNHH-1
HNHH-2
B
Percent Alive Adults
100%
75%
50%
25%
0%
Control, n>200
Ataxin-3(SCA3)-Intact, n>200
Ataxin-3(SCA3)-HNHH, n>200
Day 1 5 9 12 17 21 25 29 33 37 41 45 49
C
elav-Gal4>
Ataxin-3(SCA3)
Intact
HNHH-1
HNHH-2
Day 1
Day 7
Day 14
Ataxin-3(SCA3)
SDS-Resistant
Ataxin-3(SCA3)
SDS-Soluble
NS
Anti-Ataxin-3 (1H9)
Anti-Tubulin
Percent SDS-Resistant Ataxin-3
Normalized to "Intact" Day 1
175%
150%
125%
100%
75%
50%
25%
0%
Intact
HNHH-1
HNHH-2

Figure 3

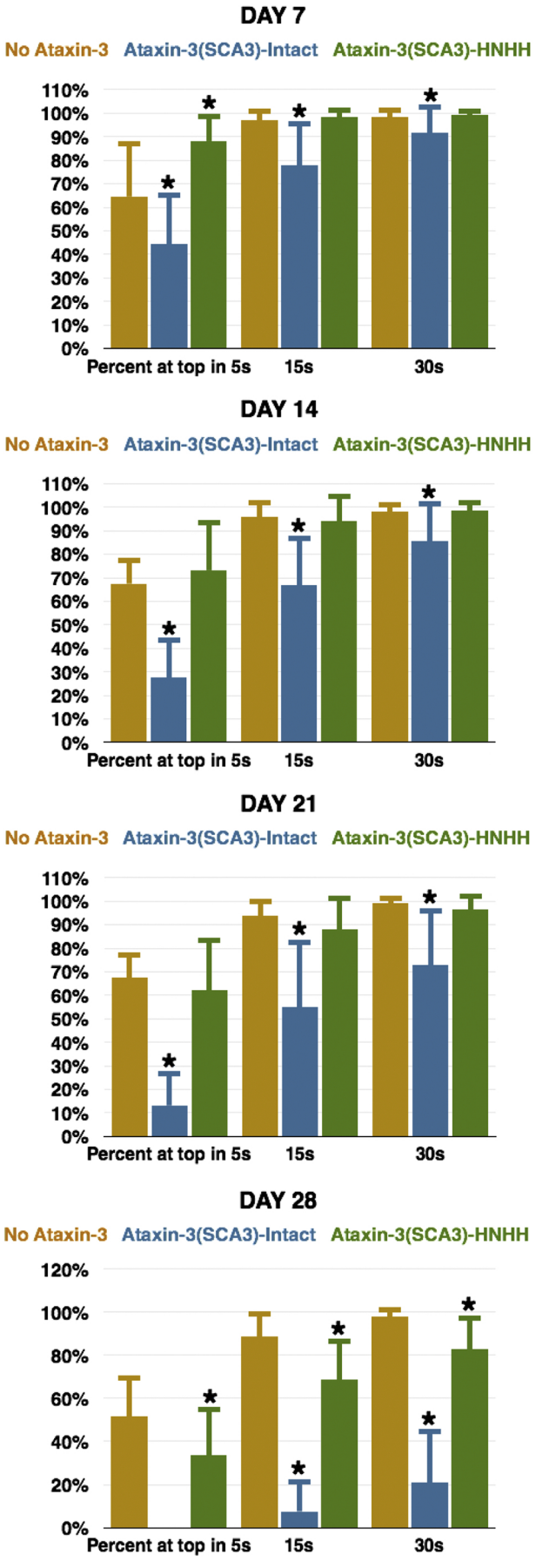
DAY 7
No Ataxin-3
Ataxin-3(SCA3)-Intact
Ataxin-3(SCA3)-HNHH
110%
100%
90%
80%
70%
60%
50%
40%
30%
20%
10%
0%
Percent at top in 5s
15s
30s
DAY 14
No Ataxin-3
Ataxin-3(SCA3)-Intact
Ataxin-3(SCA3)-HNHH
110%
100%
90%
80%
70%
60%
50%
40%
30%
20%
10%
0%
Percent at top in 5s
15s
30s
DAY 21
No Ataxin-3
Ataxin-3(SCA3)-Intact
Ataxin-3(SCA3)-HNHH
110%
100%
90%
80%
70%
60%
50%
40%
30%
20%
10%
0%
Percent at top in 5s
15s
30s
DAY 28
No Ataxin-3
Ataxin-3(SCA3)-Intact
Ataxin-3(SCA3)-HNHH
120%
100%
80%
60%
40%
20%
0%
Percent at top in 5s
15s
30s

Figure 4

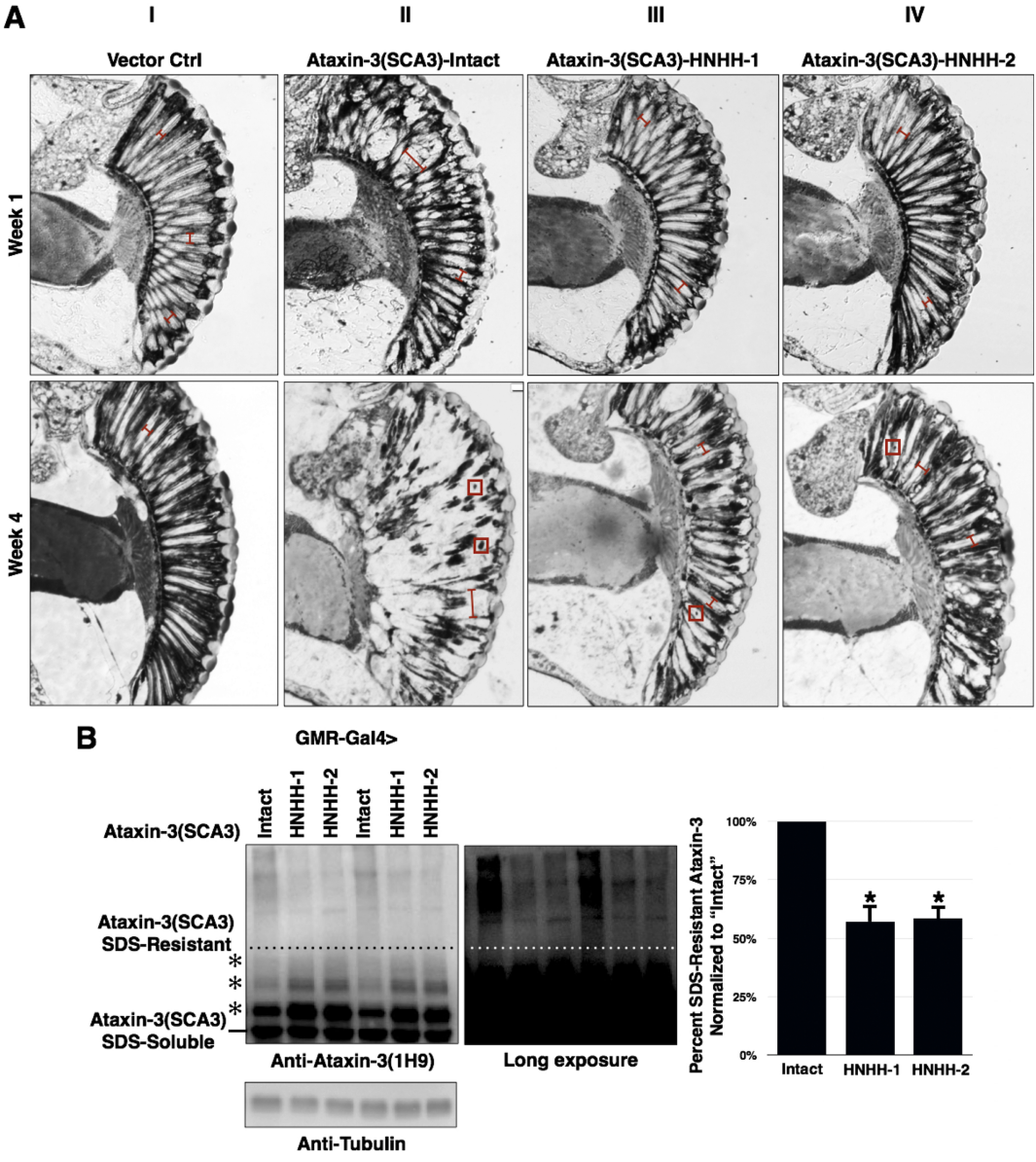
A
I
II
III
IV
Vector Ctrl
Ataxin-3(SCA3)-Intact
Ataxin-3(SCA3)-HNHH-1
Ataxin-3(SCA3)-HNHH-2
Week 1
Week 4
B
GMR-Gal4>
Intact
HNHH-1
HNHH-2
Intact
HNHH-1
HNHH-2
Ataxin-3(SCA3)
Ataxin-3(SCA3)
SDS-Resistant
Ataxin-3(SCA3)
SDS-Soluble
Anti-Ataxin-3(1H9)
Long exposure
Anti-Tubulin
Percent SDS-Resistant Ataxin-3
Normalized to "Intact"
100%
75%
50%
25%
0%
Intact
HNHH-1
HNHH-2

Figure 5

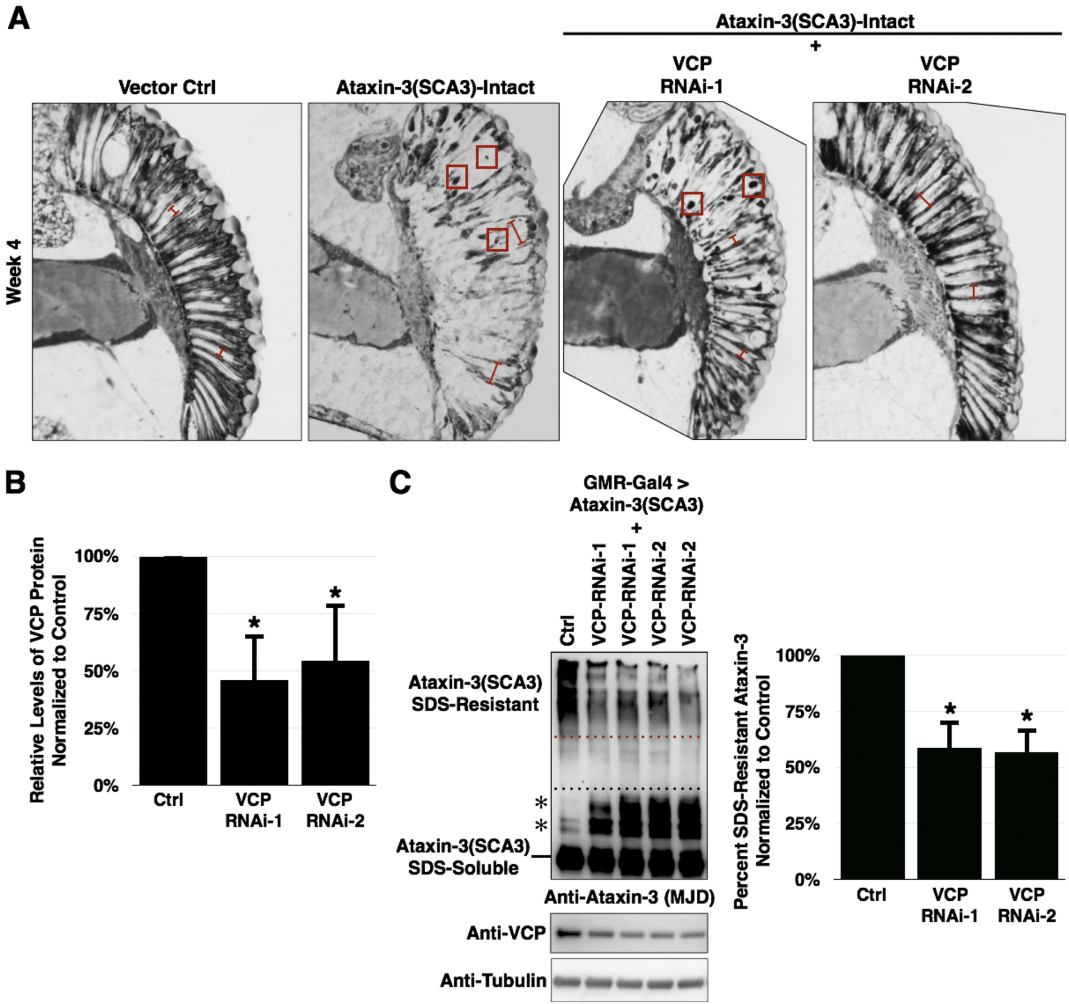
A
Ataxin-3(SCA3)-Intact
+
Vector Ctrl
Ataxin-3(SCA3)-Intact
VCP RNAi-1
VCP RNAi-2
Week 4
B
Relative Levels of VCP Protein Normalized to Control
100%
75%
50%
25%
0%
Ctrl
VCP RNAi-1
VCP RNAi-2
C
GMR-Gal4 > Ataxin-3(SCA3)
+
Ctrl
VCP-RNAi-1
VCP-RNAi-1
VCP-RNAi-2
VCP-RNAi-2
Ataxin-3(SCA3) SDS-Resistant
Ataxin-3(SCA3) SDS-Soluble
Anti-Ataxin-3 (MJD)
Anti-VCP
Anti-Tubulin
Percent SDS-Resistant Ataxin-3 Normalized to Control
100%
75%
50%
25%
0%
Ctrl
VCP RNAi-1
VCP RNAi-2

Figure 6

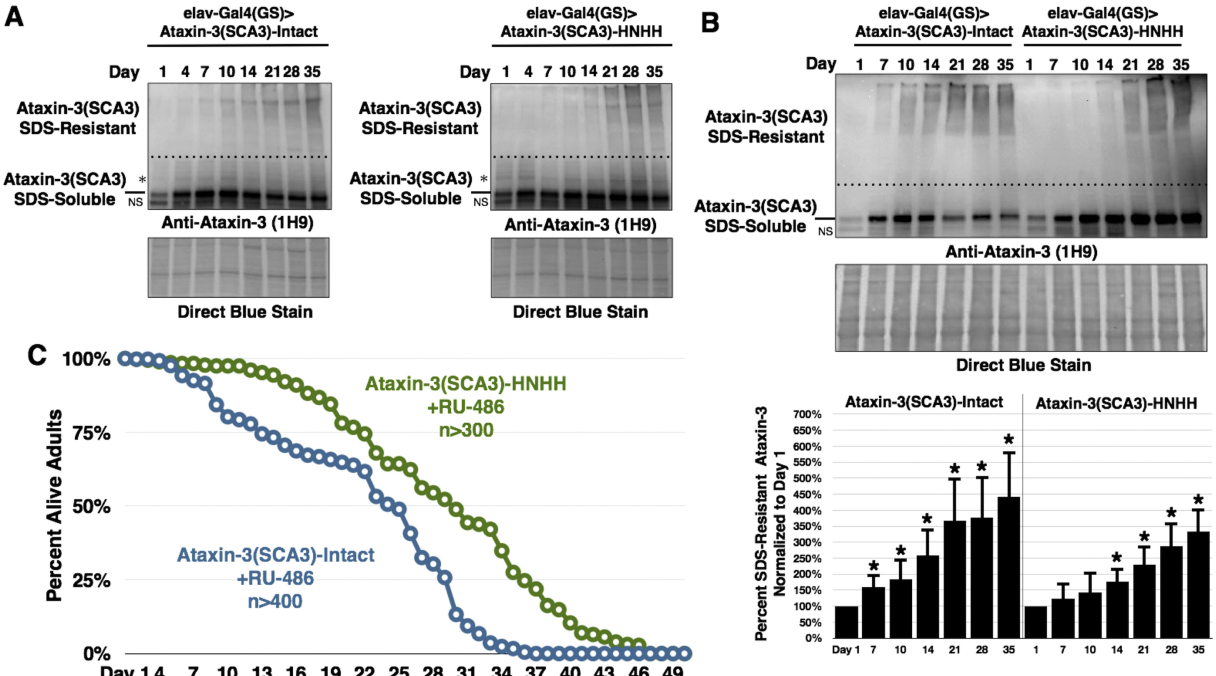
A
elav-Gal4(GS)>
Ataxin-3(SCA3)-Intact
elav-Gal4(GS)>
Ataxin-3(SCA3)-HNHH
Day 1 4 7 10 14 21 28 35
Ataxin-3(SCA3)
SDS-Resistant
Ataxin-3(SCA3)
SDS-Soluble
*
NS
Anti-Ataxin-3 (1H9)
Direct Blue Stain
B
elav-Gal4(GS)>
Ataxin-3(SCA3)-Intact
elav-Gal4(GS)>
Ataxin-3(SCA3)-HNHH
Day 1 7 10 14 21 28 35 1 7 10 14 21 28 35
Ataxin-3(SCA3)
SDS-Resistant
Ataxin-3(SCA3)
SDS-Soluble
NS
Anti-Ataxin-3 (1H9)
Direct Blue Stain
C
100%
75%
50%
25%
0%
Percent Alive Adults
Ataxin-3(SCA3)-HNHH
+RU-486
n>300
Ataxin-3(SCA3)-Intact
+RU-486
n>400
Day 1 4 7 10 13 16 19 22 25 28 31 34 37 40 43 46 49
Ataxin-3(SCA3)-Intact
Ataxin-3(SCA3)-HNHH
Percent SDS-Resistant Ataxin-3
Normalized to Day 1
700%
650%
600%
550%
500%
450%
400%
350%
300%
250%
200%
150%
100%
50%
0%
Day 1 7 10 14 21 28 35 1 7 10 14 21 28 35

Figure 7

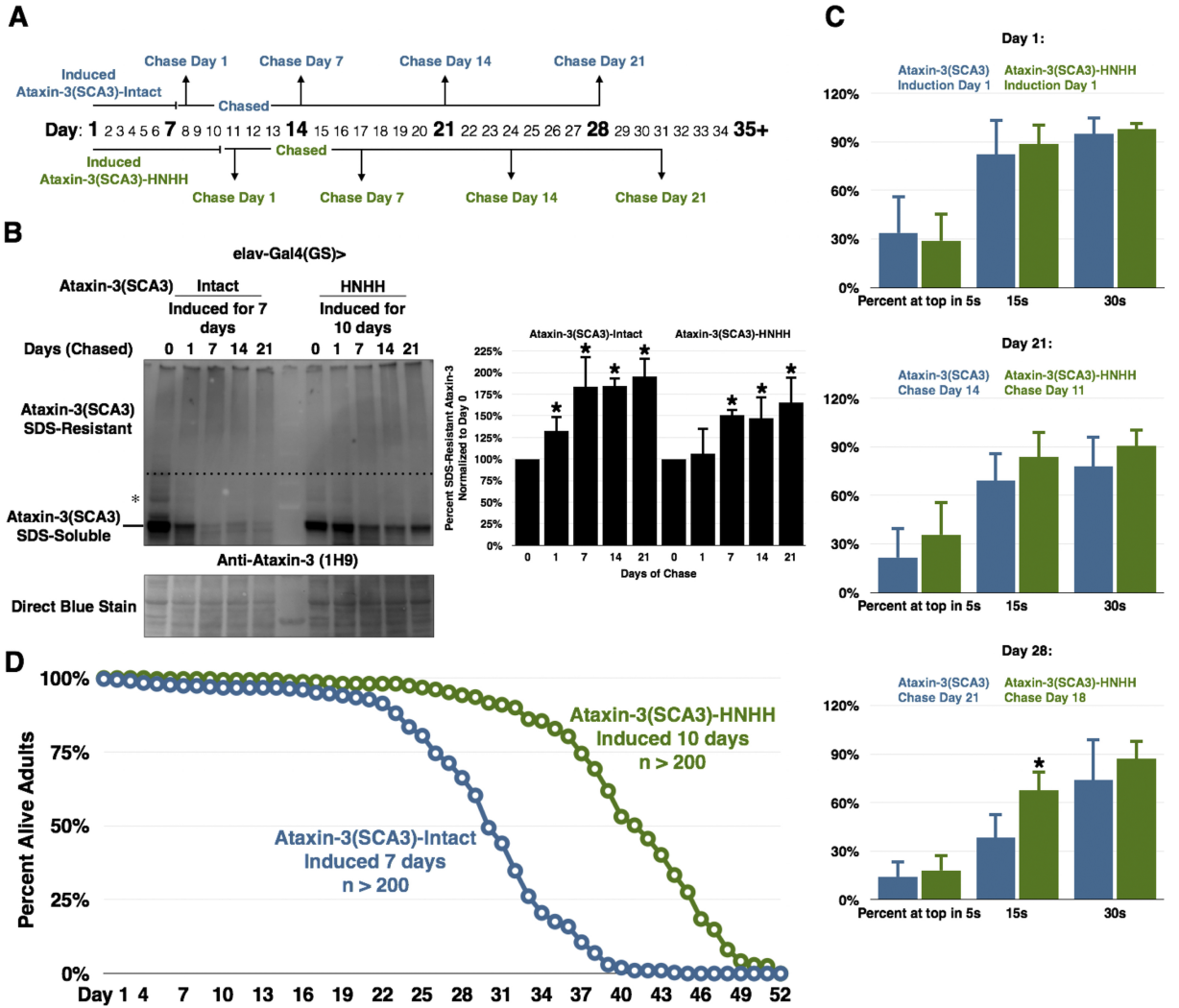
A
Induced
Ataxin-3(SCA3)-Intact
Chase Day 1
Chase Day 7
Chase Day 14
Chase Day 21
Chased
Day: 1 2 3 4 5 6 7 8 9 10 11 12 13 14 15 16 17 18 19 20 21 22 23 24 25 26 27 28 29 30 31 32 33 34 35+
Induced
Ataxin-3(SCA3)-HNHH
Chased
Chase Day 1
Chase Day 7
Chase Day 14
Chase Day 21
B
elav-Gal4(GS)>
Ataxin-3(SCA3)
Intact
Induced for 7 days
HNHH
Induced for 10 days
Days (Chased)
0 1 7 14 21 0 1 7 14 21
Ataxin-3(SCA3) SDS-Resistant
Ataxin-3(SCA3) SDS-Soluble
*
Anti-Ataxin-3 (1H9)
Direct Blue Stain
Ataxin-3(SCA3)-Intact
Ataxin-3(SCA3)-HNHH
Percent SDS-Resistant Ataxin-3 Normalized to Day 0
225%
200%
175%
150%
125%
100%
75%
50%
25%
0%
0 1 7 14 21 0 1 7 14 21
Days of Chase
C
Day 1:
Ataxin-3(SCA3) Induction Day 1
Ataxin-3(SCA3)-HNHH Induction Day 1
120%
90%
60%
30%
0%
Percent at top in 5s
15s
30s
Day 21:
Ataxin-3(SCA3) Chase Day 14
Ataxin-3(SCA3)-HNHH Chase Day 11
120%
90%
60%
30%
0%
Percent at top in 5s
15s
30s
Day 28:
Ataxin-3(SCA3) Chase Day 21
Ataxin-3(SCA3)-HNHH Chase Day 18
120%
90%
60%
30%
0%
Percent at top in 5s
15s
30s
D
Percent Alive Adults
100%
75%
50%
25%
0%
Ataxin-3(SCA3)-HNHH Induced 10 days n > 200
Ataxin-3(SCA3)-Intact Induced 7 days n > 200
Day 1 4 7 10 13 16 19 22 25 28 31 34 37 40 43 46 49 52

Figure 8

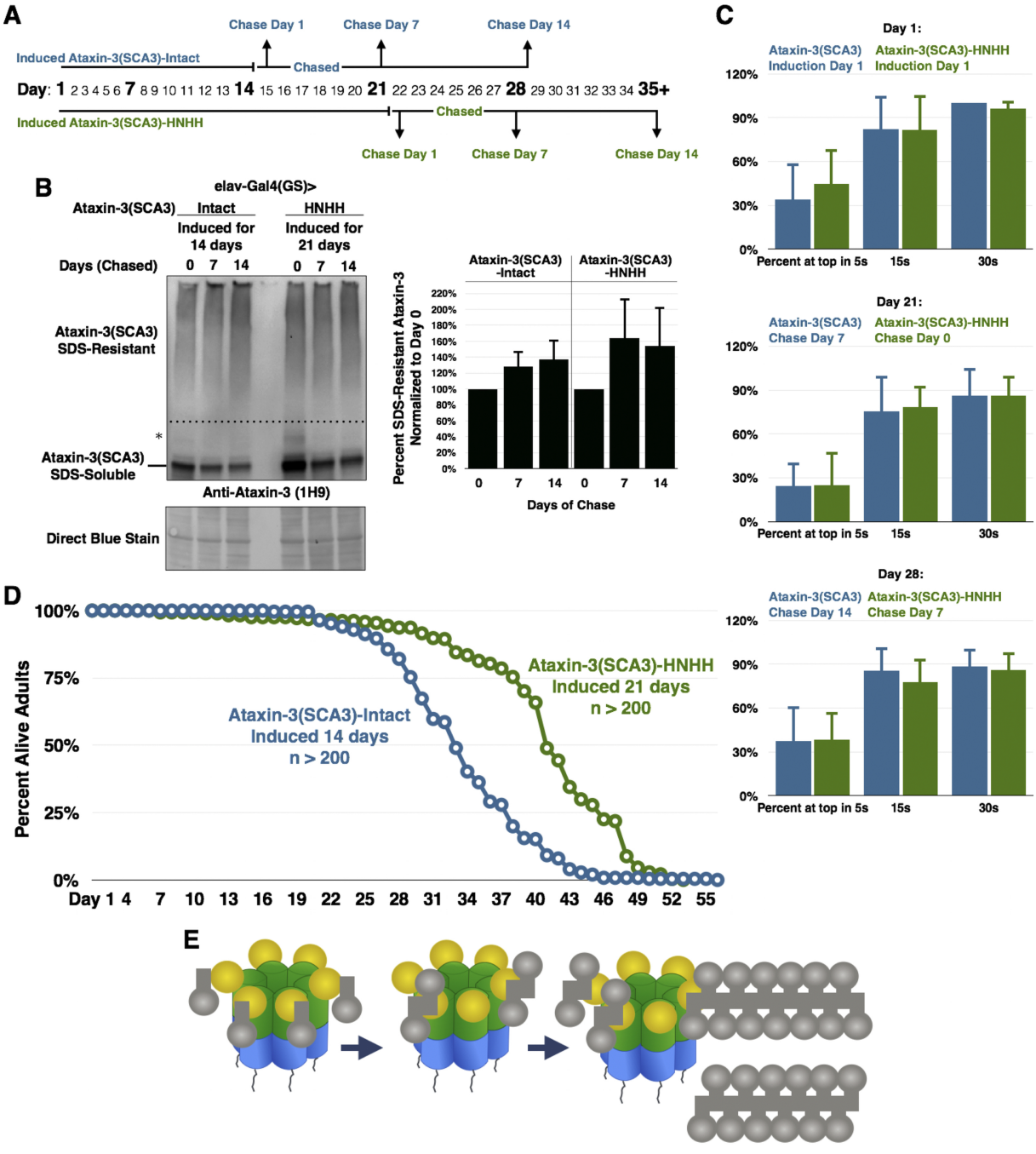
A
Chase Day 1
Chase Day 7
Chase Day 14
Induced Ataxin-3(SCA3)-Intact
Chased
Day: 1 2 3 4 5 6 7 8 9 10 11 12 13 14 15 16 17 18 19 20 21 22 23 24 25 26 27 28 29 30 31 32 33 34 35+
Induced Ataxin-3(SCA3)-HNHH
Chased
Chase Day 1
Chase Day 7
Chase Day 14
B
elav-Gal4(GS)>
Ataxin-3(SCA3)
Intact
HNHH
Induced for 14 days
Induced for 21 days
Days (Chased)
0 7 14 0 7 14
Ataxin-3(SCA3) SDS-Resistant
*
Ataxin-3(SCA3) SDS-Soluble
Anti-Ataxin-3 (1H9)
Direct Blue Stain
Ataxin-3(SCA3) -Intact
Ataxin-3(SCA3) -HNHH
Percent SDS-Resistant Ataxin-3 Normalized to Day 0
220%
200%
180%
160%
140%
120%
100%
80%
60%
40%
20%
0%
0 7 14 0 7 14
Days of Chase
C
Day 1:
Ataxin-3(SCA3) Induction Day 1
Ataxin-3(SCA3)-HNHH Induction Day 1
120%
90%
60%
30%
0%
Percent at top in 5s
15s
30s
Day 21:
Ataxin-3(SCA3) Chase Day 7
Ataxin-3(SCA3)-HNHH Chase Day 0
120%
90%
60%
30%
0%
Percent at top in 5s
15s
30s
Day 28:
Ataxin-3(SCA3) Chase Day 14
Ataxin-3(SCA3)-HNHH Chase Day 7
120%
90%
60%
30%
0%
Percent at top in 5s
15s
30s
D
Percent Alive Adults
100%
75%
50%
25%
0%
Day 1 4 7 10 13 16 19 22 25 28 31 34 37 40 43 46 49 52 55
Ataxin-3(SCA3)-Intact
Induced 14 days
n > 200
Ataxin-3(SCA3)-HNHH
Induced 21 days
n > 200
E

Figure 9